Chemopreventive Effects of Ricinus communis Metabolites in Experimental Breast Carcinogenesis via Modulation of Inflammatory and Proliferative Signaling Pathways

Mona A. Mohammed

monaarafamohammed@yahoo.com

National Research Centre

Bassant M.M. Ibrahim

National Research Centre

Noha E. Ibrahim

National Research Centre (NRC)

Marwa E. Shabana

National Research Centre

Ahmed A. El-Rashedy

University of Sadat City

Research Article

Keywords: 7,12-dimethylbenz(a) anthracene, Breast cancer, PPARα, PI3K, and STAT3, Ricinus communis, metabolomics

Posted Date: June 24th, 2026

DOI: https://doi.org/10.21203/rs.3.rs-9890166/v1

Additional Declarations: No competing interests reported.

Title: Chemopreventive Effects of *Ricinus communis* Metabolites in Experimental Breast Carcinogenesis via Modulation of Inflammatory and Proliferative Signaling Pathways.

Mona A. Mohammed[1*], Bassant M.M. Ibrahim[2], , Noha E. Ibrahim[3], Marwa E. Shabana[4], Ahmed A. El-Rashedy[5,6]

[1]Medicinal and Aromatic Plants Research Department, Pharmaceutical and Drug Industries Research Institute, National Research Centre, Giza Egypt
[2]Pharmacology Department, Medical Research and Clinical Studies Institute, National Research Centre, Dokki Giza, PO:12622. Affiliation ID60014618
[3]Microbial Biotechnology Department, Genetic Engineering and Biotechnology Division, National Research Centre (NRC), Dokki, Cairo, 12622 Egypt
[4]Pathology Department, Medical Research and Clinical Studies Institute, National Research Centre, Giza, Egypt.
5Natural and Microbial Products Department, National Research Center (NRC),
[6]Egypt Department Organic and Medicinal Chemistry, Faculty of Pharmacy, University of Sadat City, Menoufia, 32897, Egypt

***Corresponding author**
Mona A. Mohammed email: moaarafamohammed@yahoo.com

Graphical Abstract

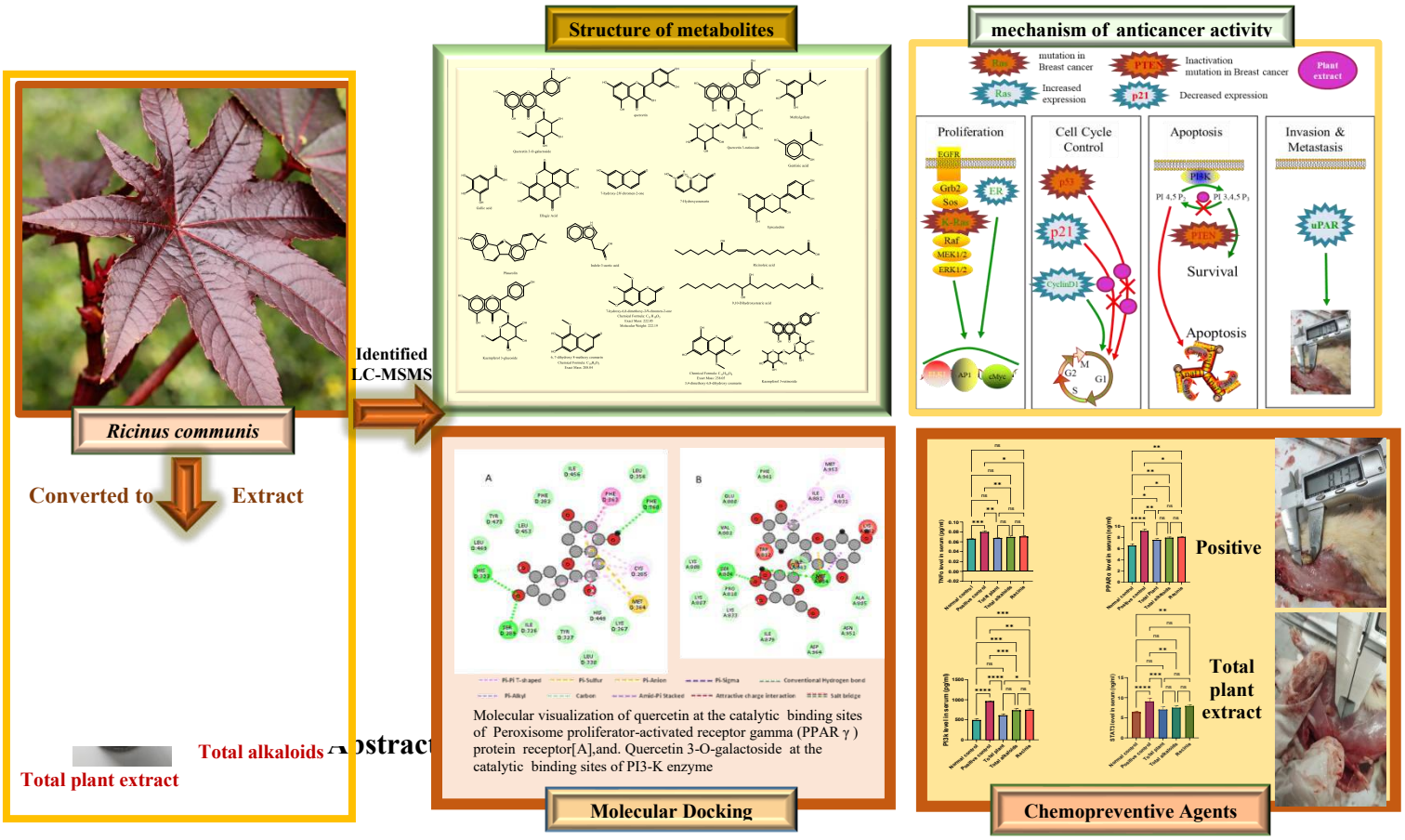

Abstract

Breast cancer remains a leading cause of cancer-related mortality worldwide, with chronic inflammation and dysregulated survival signalling contributing to tumour progression and therapeutic resistance. *Ricinus communis* is a medicinal plant widely used in traditional medicine and recognized as a rich source of biologically active alkaloids and phenolic metabolites with documented anti-inflammatory and antioxidant properties, making it a promising candidate for cancer chemoprevention. Although the fruit extract of *R. communis* has previously demonstrated anticancer activity, the chemopreventive potential of its leaf alkaloid fraction and isolated ricinine remains insufficiently explored. In this study, we investigated the anticancer and immunomodulatory effects of *R. communis* leaf total extract, total alkaloid fraction, and isolated ricinine in a DMBA/MPA-induced breast carcinogenesis model in female Sprague–Dawley rats. LC–MS/MS metabolomic profiling tentatively identified 37 secondary metabolites, including alkaloids, flavonoids, phenolic acids, and coumarins, with ricinine as the predominant alkaloid. Three putative pyridone alkaloid derivatives (methyl 5-(2-oxo-1,2-dihydropyridin-4-yl)pentanoate, methyl 5-(3-cyano-2-oxo-1,2-dihydropyridin-4-yl)pentanoate and 1-methyl-2-oxo-dihydropyridine-3-carbonitrile) spentanoate, and 1-methyl-2-oxo-dihydropyridine-3-carbonitrile) were tentatively characterized, expanding the phytochemical profile and suggesting previously unexplored anticancer chemotypes. Biological evaluation revealed significant suppression of tumour development and restoration of mammary histoarchitecture in treated groups. Histopathological analysis confirmed reduced malignancy and improved stromal organisation. Mechanistically, treatment markedly downregulated TNF-α, PI3K, and STAT3 while modulating PPARα signalling pathways. Molecular docking further supported strong binding interactions with PI3K and PPAR targets, highlighting *R. communis* alkaloids as promising multi-target chemopreventive agents against inflammation-associated breast carcinogenesis.

Keywords: 7,12-dimethylbenz(a) anthracene, Breast cancer, PPARα, PI3K, and STAT3, *Ricinus communis, metabolomics.*

1. Introduction

Cancer remains one of the leading causes of mortality worldwide and continues to represent a major global public health challenge. A principal limitation in successful cancer therapy is the development of multidrug resistance (MDR), in which cancer cells acquire defensive mechanisms that reduce the efficacy of chemotherapeutic agents. These resistance pathways include enhanced drug efflux, alterations in apoptotic signaling, metabolic reprogramming, and increased cellular detoxification, ultimately leading to treatment failure and poor patient prognosis. Among different malignancies, breast cancer remains the most frequently diagnosed cancer and one of the leading causes of cancer-related deaths among women worldwide. High mortality rates have been particularly reported in several African countries, including Western Africa [1]. Despite major advances in chemotherapy and hormone-based therapies, resistance to treatment remains a substantial obstacle in breast cancer management. Aromatase, a key enzyme involved in estrogen biosynthesis, is highly expressed in hormone-dependent breast cancers. Consequently, aromatase inhibitors have represented a cornerstone in breast cancer therapy for more than four decades. Nevertheless, currently available drugs are often associated with adverse

effects, toxicity, and the eventual development of resistance, highlighting the urgent need for safer and more effective therapeutic alternatives [2]. In this context, natural products have attracted increasing attention as promising sources of anticancer agents due to their structural diversity, multitarget mechanisms, lower toxicity, and affordability. Importantly, many phytochemicals are capable of modulating several molecular pathways simultaneously, thereby overcoming mechanisms associated with multidrug resistance. Fitarget activities that may help overcome drug-resistance pathways in cancer cells. Therefore, the discovery of new natural sources rich in bioactive alkaloids remains an important strategy for the development of innovative anticancer therapies. Among medicinal plants, *Ricinus communis* (family Euphorbiaceae) has attracted considerable scientific interest because of its broad spectrum of biological activities and rich phytochemical composition. The plant is widely distributed and has long been recognized for its medicinal and industrial importance [3]. Previous phytochemical investigations demonstrated that different parts of the plant contain diverse classes of secondary metabolites, including alkaloids, flavonoids, tannins, triterpenes, coumarins, and other phenolic compounds. Several studies have also reported antioxidant, anti-inflammatory, antimicrobial, hepatoprotective, and anticancer activities for Ricinus communis extracts, supporting its therapeutic relevance as a medicinal resource [4, 5]. Despite these promising biological properties, most previous studies on Ricinus communis relied mainly on conventional phytochemical screening, targeted compound isolation, and classical structural elucidation techniques rather than comprehensive metabolomic investigations. Earlier studies primarily focused on the identification of selected alkaloids and flavonoids using traditional analytical approaches [4]. However, advanced metabolomics technologies, particularly liquid chromatography coupled with high-resolution mass spectrometry (LC-HRMS/MS), now provide powerful tools for the comprehensive characterization of plant metabolites and the elucidation of biochemical pathways associated with pharmacological activity. Such approaches enable the detection of structurally diverse metabolites, including low-abundance bioactive compounds that may contribute significantly to therapeutic efficacy. Accordingly, metabolomics-driven investigations are essential for exploring the chemical diversity of *Ricinus communis* and identifying novel bioactive metabolites with potential anticancer activity. Particular emphasis should be directed toward alkaloid-rich fractions, as alkaloids remain among the most successful natural-product-derived anticancer agents reported to date. Therefore, the present study aims to investigate *Ricinus communis* and its alkaloid-rich fractions, particularly recinine and total alkaloids, as potential prophylactic and therapeutic natural agents capable of suppressing breast cancer progression in an experimentally induced rat model that mimics breast cancer in female patients. This work further seeks to provide comprehensive metabolomic insights into the plant's chemical composition and to explore its potential as a promising natural source of novel anticancer alkaloids.

2. Materials and methods

2.1. Materials

Plant extraction: Red fresh leaves of *Ricinus communis* L. (3 kg) were collected in 2025 from a private farm. The leaves were washed with distilled water to remove surface contaminants, air-dried in the shade at room temperature until constant weight, then ground into a coarse powder and stored in airtight containers. The powdered material was exhaustively extracted with absolute methanol until the solvent became colorless. The combined extracts were concentrated

under reduced pressure using a rotary evaporator, yielding 280 g of a dark green semisolid total extract [6].

Animals: Forty adult female Sprague-Dawley rats (180–200 g) were obtained from the animal facility of the (NRC), Egypt. Animals were maintained under standard laboratory conditions with free access to food and water and acclimated for two weeks prior to the experiment [9]. All procedures adhered to the National Regulations of Animal Welfare and were approved by the Institutional Animal Ethical Committee (IAEC) and the Medical Research Ethics Committee of NRC (MREC, protocol no. 0-8-3).

Chemicals: Dichloromethane, thiopental sodium, formaldehyde, sodium chloride, 7,12-dimethylbenz(a)anthracene (DMBA), and medroxyprogesterone acetate (MPA) were purchased from Sigma-Aldrich (USA).

Biochemical assay Kits: Enzyme linked immunosorbent assay kits (Elisa), for detection of the levels of: peroxisome proliferator-activated receptor alpha (PPARα), signal transducer and activator of transcription 3 (STAT3), phosphoinositide 3-kinase (PI3K), and tumour necrosis factor alpha (TNFα). The kits were purchased from MYBiosourse company (Southern California, San Diego (USA)).

2.2. Methods

Extraction of total Alkaloids**: 1)** 100 g portion of the crude extract was subjected to liquid–liquid partitioning between dichloromethane and water to obtain the total alkaloid fraction. The crude extract and dichloromethane layer were separately evaporated to dryness and weighed. The dried material was then dissolved in 1% hydrochloric acid solution and transferred to a separatory funnel. The acidic solution was repeatedly extracted with chloroform until the organic phase became clear, and these chloroform extracts were discarded. The remaining aqueous layer was filtered and rendered alkaline by adding ammonia solution to adjust the pH to 10–11. The basified solution was subsequently extracted several times with chloroform, and the combined organic layers were evaporated to dryness to obtain the total alkaloids. Alkaloid presence was confirmed using Dragendorff's reagent following a standard qualitative procedure [7].

Isolation of the alkaloid recinine*:* recinine was isolated from the total alkaloid fraction by silica gel column chromatography. Before packing, the silica gel was pretreated with a small amount of ammonia to minimize retention of basic constituents. Approximately 3 g of the alkaloid extract was dissolved in a small volume of chloroform and applied to the column. Elution was initially performed with chloroform, followed by gradual polarity enhancement through the addition of 1% methanol after every 250 mL of solvent. Fractions (50 mL each) were collected and monitored by thin-layer chromatography using dichloromethane–methanol (9.5:0.5, v/v) as the mobile phase. Fractions exhibiting similar TLC patterns were pooled, and alkaloid presence was verified using Dragendorff's reagent. The fraction containing recinine was further purified and dried for structural identification.

LC-MSMS and NMR: liquid chromatography–tandem mass spectrometry (UPLC–MS/MS) analyses were performed on a Waters Acquity system coupled to a Thermo Q-Exactive quadrupole–Orbitrap mass spectrometer. Separation used a BEH Shield C18 column (150 × 2.1 mm, 1.7 μm) with water + 0.1% formic acid (A) and acetonitrile (B) at 0.4 mL/min. The gradient ran 5–50% B (0–15 min), 50–98% B (15–22 min), held 5 min, then returned to initial conditions with 3 min re-equilibration. Heated electrospray ionization was applied in positive and negative modes (±3 kV) with sheath gas 48 L/min, auxiliary gas 13 L/min, capillary 250 °C, auxiliary

heater 380 °C, and CID 15 eV [7]. NMR spectra were recorded at 400 MHz (^{1}H) and 101 MHz (^{13}C) in $CDCl_3$ on a Bruker Avance III spectrometer. Chemical shifts were referenced to residual solvent signals. 2D experiments (COSY, HSQC, HMBC) are used.

Study Design: The involved rats were kept in the same housing conditions throughout the experiment and received the same care and diet.

Induction of breast cancer: Thirty-two mature female SD rats were given a single dose of 20 mg/kg of DMBA in 1 mL of olive oil by gavage (PO) and repeated injections every other day of MPA by intra muscular (IM) administration for 8 successive weeks [8, 9]. The rats were examined once weekly for apparent changes in mammary gland appearance that might denote carcinogenesis, until changes in the form of red prominent nipples with underlying induration appeared. Twenty-three rats developed these signs, the rats that didn't show these signs were excluded from the experiment. Three rats were subjected to mastectomy and the breast glands were histopathologically examined to confirm or exclude the development of breast cancer.

Animal groups: Twenty rats were enrolled in the study were equally divided into five groups (5 rats each).

1st group: Normal Control: The animals were allowed free chow and water access throughout the experimental duration without any intervention.

2nd group: Positive control for which induction of animal model mimicking breast cancer was done by single oral administration of DMBA in addition to IM administration of MPA to SD rats [8, 9].

3rd-5th groups: Breast cancer suffering rats were treated by oral administration of recinine (5 mg/kg), total alkaloids (5 mg/kg) and total plant extract (10 mg/kg [10] respectively, for 8 weeks.

Blood samples collection and processing: At the end of the experiment (after 16 weeks), blood samples were withdrawn from the retro-orbital venous plexus of veins, under general anaesthesia using thiopental sodium (50 mg/kg) that was administered intra-peritoneally (IP) [11], rats had been deprived of food but allowed free access to water for 12 hours before collecting blood samples. Collected blood samples were allowed to stand for 10 min at room temperature then centrifuged at 4°c using cooling centrifuge (Laborezentrifugen, 2k15, Sigma, Germany) at 2500 r.p.m for 10 minutes, then the sera were separated for the assessment of serum levels of PPARα, STAT3, PI3K, and TNFα following manufacturer's guidelines.

Macroscopic examination*:* Immediately following blood sampling, the rats were sacrificed by decapitation while still under general anaesthesia. The breast glands were excised and the tumour sizes were measured by using digital caliber.

Histopathology: Mammary gland tissues were collected and fixed in 4% paraformaldehyde for 24 h, rinsed with distilled water, and dehydrated through graded ethanol (70–100%), cleared in xylene, and embedded in paraffin. Sections of 4–5 μm were mounted on glass slides, dewaxed, and stained with hematoxylin and eosin. Histological changes were examined using an Olympus CX41 light microscope, and photomicrographs were captured and processed with Adobe Photoshop v8.0.

Statistical Analysis: Tumor dimensions were analyzed using two-way ANOVA with Tukey-Kramer's post hoc test ($P \leq 0.05$). Biochemical assay data were evaluated using one-way ANOVA followed by Tukey-Kramer's test ($P \leq 0.001$). All analyses were performed using GraphPad Prism v9 [14].

Molecular modeling: **Molecular Modeling:** *In silico* docking studies were conducted using AutoDock Vina [12]. Ligands were chosen based on LC–MS/MS analysis, representing the 33

major compounds identified in the plant extract. The 3D structures of Peroxisome Proliferator-Activated Receptor Gamma (PPARγ, PDB ID: 1FM9) [13] and PI3-Kinase (PDB ID: 2CHX) [14] were obtained from the RCSB Protein Data Bank (https://www.rcsb.org/) [15]. The structures of the compounds synthesized were drawn using ChemOffice tool (ChemD. Compound structures were drawn in ChemDraw 16.0 and converted into 3D geometries; their energies were minimized using ChemBio3D before docking. Proteins were prepared by removing co-crystallized ligands, water molecules, and cofactors, retaining essential residues, following standard protocols in AutoDock 4.2 (MGLTools 1.5.6). The docking grid was defined to encompass the active site region. AutoDock Vina v.1.2.0 was used to generate up to nine conformations per ligand. Resulting poses were analyzed in BIOVIA Discovery Studio to visualize interactions with binding-site residues, and the best-scoring conformers showing meaningful ligand–protein contacts were selected for further interpretation [16].

3. Results

3.1. Phytochemistry studies

Identification of Compound*:* The isolated compound was identified as ricinine, the major pyridone alkaloid of *Ricinus communis*. The ^{1}H NMR spectrum (401 MHz, $CDCl^{3}$) displayed two ortho-coupled aromatic protons at δ 7.53 (d, J = 7.7 Hz, 1H, H-6) and δ 6.07 (d, J = 7.7 Hz, 1H, H-5), a methoxy singlet at δ 3.99 (s, 3H, OCH_3), an N-methyl singlet at δ 3.55 (s, 3H, N–CH_3), and a weak singlet at δ 1.63 (s, 1H, exchangeable proton). The ^13C NMR spectrum (101 MHz, $CDCl_3$) exhibited characteristic signals at δ 172.50 (C=O, C-2), 161.42 (C-4), 143.66 (C-6), 113.81 (C-5), 93.69 (C-3), and 88.76 (C-1), together with δ 57.26 (OCH_3) and 37.72 (N–CH_3). Solvent signals of $CDCl_3$ appeared at δ 77.48, 77.36, 77.16, and 76.84. In addition to the ^{1}H and ^{13}C NMR spectra, two-dimensional NMR experiments were recorded, including COSY, HSQC, and HMBC. The ^{1}H–^{1}H COSY spectrum confirmed the ortho coupling between the aromatic protons H-5 and H-6. The HSQC spectrum showed direct one-bond correlations between all proton and carbon signals, allowing unambiguous assignment of protonated carbons, including the methoxy and N-methyl groups. The HMBC spectrum displayed key long-range correlations from the aromatic protons and methyl groups to adjacent quaternary carbons, particularly the carbonyl and heteroaromatic carbons of the pyridone ring, supporting the substitution pattern of the molecule. On the basis of these spectroscopic data in figures S(1-5), the compound was confirmed as ricinine (3-cyano-4-methoxy-N-methyl-2-pyridone).

LC–MS/MS Metabolite Profiling: LC–MS/MS analysis of the *Ricinus communis* extract resulted in the identification of 37 metabolites belonging to several major chemical classes, including pyridone alkaloids, phenolic acids, flavonoids, coumarins, fatty acids, tocopherols, diterpenes, indole derivatives, and dicarboxylic acids. Metabolite annotation was achieved based on accurate mass measurements, retention times, MS/MS fragmentation patterns acquired in both negative and positive ESI modes, and comparison with previously reported data. Ricinine was further confirmed by NMR spectroscopy. All identified metabolites were detected in the total plant extract, while pyridone alkaloids were markedly enriched in the alkaloid fraction in Figure (S6**).**

Pyridone alkaloids represented the dominant class of nitrogen-containing metabolites detected in *R. communis*. These compounds are characteristic secondary metabolites of the genus and were mainly detected in the early retention time region. Identified pyridone alkaloids included 1-methylpyridin-2(1H)-one (C_6H_7NO)**,** 1,3-dimethylpyridin-2(1H)-one (C_7H_9NO)**,** N-demethylricinine ($C_7H_6N_2O_2$)**,** ricinidine ($C_7H_6N_2O$)**,** ricinine ($C_8H_8N_2O_2$)**,** harmane ($C_{12}H_{10}N_2$)**,**

1-methyl-4-(4-methylpentyloxy)-5,6-dihydropyridin-2(1H)-one ($C_{12}H_{21}NO_2$)**,** and methyl 5-(3-cyano-1-methyl-2-oxo-1,2-dihydropyridin-4-yl)pentanoate ($C_{13}H_{16}N_2O_3$)**.** Notably, three pyridone alkaloids are reported here for the first time in *R. communis*. These newly detected compounds are methyl 5-(2-oxo-1,2-dihydropyridin-4-yl)pentanoate ($C_{11}H_{15}NO_3$)**,** methyl 5-(3-cyano-2-oxo-1,2-dihydropyridin-4-yl)pentanoate ($C_{12}H_{14}N_2O_3$)**,** and 1-methyl-2-oxo-dihydropyridine-3-carbonitrile ($C_7H_8N_2O$)**.** These compounds were characterized by their accurate precursor ions at *m/z* 210.1123–210.1125, 235.1074–235.1077, and 137.0710–137.0709, respectively, with MS/MS spectra showing diagnostic fragment ions consistent with pyridone skeletons and cyano-substituted derivatives. Overall, MS/MS fragmentation of pyridone alkaloids was dominated by neutral losses of CN, CO, CH_3, and alkyl side chains, supporting the structural assignments. Ricinine was isolated and unambiguously confirmed by NMR spectroscopy, further validating the LC–MS/MS-based identification strategy in Table 1.

Phenolic acids constituted an important group of polar metabolites in the extract. Identified compounds included gallic acid ($C_7H_6O_5$)**,** gentisic acid ($C_7H_6O_4$)**,** methyl gallate ($C_8H_8O_5$)**,** and ellagic acid ($C_{14}H_6O_8$)**.** Their MS/MS spectra showed characteristic decarboxylation and dehydration losses, yielding stable phenoxide ions typical for hydroxybenzoic acid derivatives.

Flavonoids and Flavonoid Glycosides: Several flavonoids were detected, either as aglycones or glycosylated forms, including epicatechin ($C_{15}H_{14}O_6$)**,** quercetin ($C_{15}H_{10}O_7$)**,** quercetin 3-O-rutinoside ($C_{27}H_{30}O_{16}$)**,** quercetin 3-O-galactoside ($C_{21}H_{20}O_{12}$)**,** kaempferol 3-rutinoside ($C_{27}H_{30}O_{15}$), and kaempferol 3-glucoside ($C_{21}H_{20}O_{11}$)**.** Fragmentation was characterized by sequential losses of sugar moieties and formation of diagnostic aglycone ions.

Coumarin derivatives detected in the extract included 6,7-dihydroxy-8-methoxy coumarin ($C_{10}H_8O_5$)**,** 7-hydroxy-6,8-dimethoxy-2H-chromen-2-one ($C_{11}H_{10}O_5$)**,** 7-hydroxycoumarin ($C_9H_6O_3$)**, and** 3,4-dimethoxy-6,8-dihydroxy coumarin ($C_{11}H_{10}O_6$)**.** Their MS/MS spectra reflected characteristic coumarin core fragmentation and methoxy group losses in Table 1.

Indole and Cinnamic Acid Derivatives: Two signaling-related metabolites were identified, namely indole-3-acetic acid ($C_{10}H_9NO_2$) and (E)-O-methoxycinnamic acid ($C_{10}H_{10}O_3$), confirmed by typical neutral losses of CO_2 and side-chain cleavage ions in Table 1.

Fatty Acids, Tocopherol, and Other Metabolites: Lipid-related constituents included ricinoleic acid ($C_{18}H_{34}O_3$)**,** 9,10-dihydroxystearic acid ($C_{18}H_{36}O_4$), and α-tocopherol ($C_{29}H_{50}O_2$). Additionally**,** kaurene ($C_{20}H_{34}$), phaseolin ($C_{20}H_{18}O_4$), pimelic acid ($C_7H_{12}O_4$), and sebacic acid ($C_{10}H_{18}O_4$) were identified, reflecting the chemical diversity of the extract in Table 1.

Table 1: LC-MS/MS profiling of *Ricinus communis* metabolites: retention time, identification, formula, exact mass, fraction distribution, and ESI fragmentation patterns.

No	RT [Min]	metabolite identification/ {Smiles}	Structure	Chemical formula	exact mass of $[M-H]^-$		exact mass of $[M-H]^{-+}$		Δ ppm	Plant Extractions		Ref.
					measured	Fragmentation	measured	Fragmentation		Total plant extract	Total alkaloids	
Pyridone alkaloids group:												
1	1.90	*1-methylpyridin-2(1H)-one* **{CN1C=CC=CC1=O}**	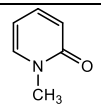	C_6H_7ON	-	-	110.0605, 110.0600	93.0580[C_6H_7N], 80.0502[C_5H_6N]	4.1855	*	*	[17]
2	2.07	*methyl 5-(2-oxo-1,2-dihydropyridin-4-yl)pentanoate* **{O=C1C=C(CCCCC(OC)=O)C=CN1}**	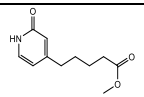	$C_{11}H_{15}NO_3$	-	-	210.1123, 210.1125	180.1013[$C_{10}H_{14}NO_2$], 146.0971[$C_{10}H_{12}N$], 107.0736[C_7H_9N]	-1.0041	*	*	new
3	2.74	*1,3-dimethylpyridin-2(1H)-one* **{CN1C=CC=C(C)C1=O}**	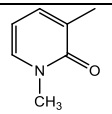	C_7H_9NO	-	-	124.0759, 124.0757	96.0814[$C_6H_{10}N$], 84.0451[C_4H_6NO]	1.9735	*	*	[17]
4	3.41	*N-demethylricinine* **{O=C1NC=CC(OC)=C1C#N}**	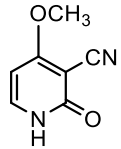	$C_7H_6N_2O_2$	-	-	151.0503, 151.0502	139.0501[$C_6H_7N_2O_2$]. 123.0556[$C_6H_7N_2O$]	0.3869	*	*	[18]
5	3.42	*methyl 5-(3-cyano-2-oxo-1,2-dihydropyridin-4-yl)pentanoate* **{O=C1C(C#N)=C(CCCCC(OC)=O)C=CN1}**	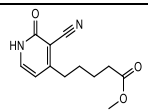	$C_{12}H_{14}O_3N_2$	-	-	235.1074, 235.1077	217.0970[$C_{12}H_{13}N_2O_2$], 203.0813[$C_{11}H_{11}N_2O_2$], 179.106[$C_9H_7N_2O_2$]	-1.4579	*	*	new
6	3.37	Ricinidine **{CN1C=CC=C(C#N)C1=O}**	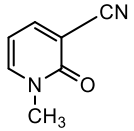	$C_7H_6N_2O$	-	-	135.0554, 135.0553	108.0448[C_6H_6NO]	1.0793	*	*	[19]
7	3.55	*1-methyl-2-oxo-dihydropyridine-3-carbonitrile* **{N#CC(CC=CN1C)C1=O}**	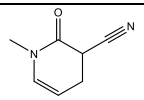	$C_7H_8ON_2$	-	-	137.0710, 137.0709	130.9857[C_7HNO_2]	0.4354	*	*	new

8	4.0	*4-methoxy-1-methyl-2-oxo-1,2-dihydropyridine-3-carboxylic acid* **{CN1C=CC(OC)=C(C(O)=O)C1=O}**	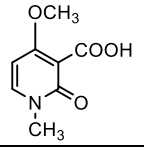	$C_8H_9NO_4$	-	-	184.0606, 184.0604	166.0863[$C_7H_{10}NO_4$], 142.0866[$C_5H_{10}NO_4$], 140.0704[$C_7H_{10}NO_2$] 124.0759[$C_7H_{10}NO$]	0.6946	*	*	[18]
9	4.66	*Ricinine* **{CN1C=CC(OC)=C(C#N)C1=O}**	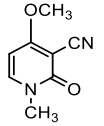	$C_8H_8O_2N_2$	-	-	165.0655, 165.0659	138.0547[$C_7H_8O_2N$], 126.0545[$C_6H_8O_2N$], 84.0449[C_4H_6ON]	-2.2937	*	*	NMR [19]
10	5.98	*Harmane* **{CN1C=CC=C(C#N)C1=O}**	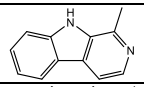	$C_{12}H_{10}N_2$	-	-	183.0911, 183.0917	155.9739, 137.0961	-3.2509	*	*	MS-Dial
11	7.95	*1-methyl-4-(4-methylpentyloxy)-5,6-dihydropyridin-2(1H)-one* **{CN1CCC(OCCCC(C)C)=CC1=O}**	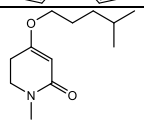	$C_{12}H_{21}O_2N$	-	-	212.1645, 212.1645	195.1384[$C_{12}H_{19}O_2^+$], 177.1274[$C_{12}H_{17}O^+$], 159.1168[$C_{12}H_{15}^+$], 149.1326[$C_{11}H_{17}^+$]	-0.0741	*	*	[20]
12	9.18	*6-Nitroimidazo[1,2-a]pyridine* **{O=[N+](C1=CN2C(C=C1)=NC=C2)[O-]}**	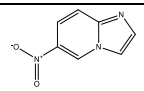	$C_7H_5N_3O_2$	162.0309, 162.0311	133.0277[$C_6H_3ON_3$],	-	-	1.2343			MS-Dial
13	9.91	*Indole-3-acetic acid* **{O=C(Cc(c[nH]1)c2c1cccc2)O}**	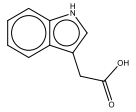	$C_{10}H_9NO_2$	174.0547, 174.0550	159.0310[$C_9H_5N_2O$], 142.0284[C_9H_4NO]	-	-	1.7235	*	-	[21]
14	10.90	*methyl 5-(3-cyano-1-methyl-2-oxo-1,2-dihydropyridin-4-yl)pentanoate* **{O=C1N(C)C=CC(CCCCC(OC)=O)=C1C#N}**	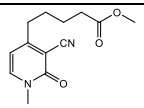	$C_{13}H_{16}N_2O_3$	-	-	249.1246, 249.1234	190.0498[$C_{10}H_8N_3O$], 149.0234[$C_8H_5O_3$], 121.0286[$C_7H_5O_2$]	4.8323	*	*	[20]
Phenolic acids, Flavonoids and Flavonoid Glycosides groups:												
15	2.95	*Gallic acid* **{OC1=CC(C(O)=O)=CC(O)=C1O}**	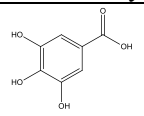	$C_7H_6O_5$	169.0130, 169.0131	125.0229	-	-	-0.8831	*	-	[22]
16	4.14	*Epicatechin* **{OC1=C(C[C@@H](O)[C@@H](C2=CC(O)=C(O)C=C2)O3)C3=CC(O)=C1}**	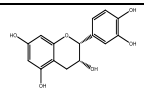	$C_{15}H_{14}O_6$	289.0719, 289.0707	245.0818[$C_{14}H_{13}O_4$], 203.0703[$C_{12}H_{11}O_3$], 179.0339[$C_9H_7O_4$], 151.0379[$C_8H_7O_3$]	-	-	4.1661	*	-	[22]

17	4.68	*Gentisic acid* **{O=C(c1c(O)ccc(O)c1)O}**	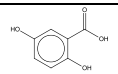	$C_7H_6O_4$	153.0180, 153.0182	109.0280[$C_6H_5O_2$]	-	-	-1.7011	*	-	[22]
18	5.19	*Methylgallate* **{COC(C1=CC(O)=C(O)C(O)=C1)=O}**	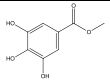	$C_8H_8O_5$	183.0288, 183.0288	168.0052[$C_7H_8O_5$], 124.0150[$C_6H_4O_4$]	-	-	-0.2021	*	-	[23]
19	5.34	*Quercetin 3-rutinoside* **{CC1O[C@H](C([C@H]([C@H]1O)O)O)OCC2O[C@H](C(C([C@@H]2O)O)O)Oc(c(c3cc(O)c(O)cc3)oc4c5c(O)cc(O)c4)c5=O}**	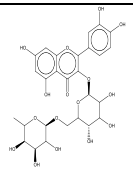	$C_{27}H_{30}O_{16}$	609.1573, 609.1570	300.0272[$C_{15}H_8O_7$]	-	-	-0.4924	*	-	[22]
20	5.43	*Quercetin 3-O-galactoside* **{O=c(c(O[C@@H]1O[C@@H]([C@@H](C(C1O)O)O)CO)c(c2cc(O)c(O)cc2)o3)c4c3cc(O)cc4O}**	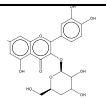	$C_{21}H_{20}O_{12}$	463.0869, 463.0871	316.0224[$C_{15}H_8O_8$], 300.0268[$C_{15}H_8O_7$]	-	-	-0.4307	*	-	[24]
21	5.63	*Kaempferol 3-rutinoside* **{CC1O[C@H](C([C@H]([C@H]1O)O)O)OCC2O[C@H](C(C([C@@H]2O)O)O)Oc(c(c3ccc(O)cc3)oc4c5c(O)cc(O)c4)c5=O}**	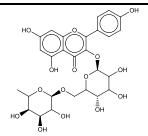	$C_{27}H_{30}O_{15}$	593.1508, 593.1511	299.0556[$C_{16}H_{11}O_6$]	-	-	0.5057	*	-	[4]
22	5.71	*6, 7-dihydroxy 8-methoxy coumarin* {O=C1OC2=C(C=C(O)C(O)=C2OC)C=C1}	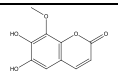	$C_{10}H_8O_5$	207.0292, 207.0288	192.0418[$C_10H_8O_4$], 179.0340[$C_9H_7O_4$], 148.0154[$C_8H_4O_3$]	-	-	2.1061	*	-	[25]
23	6.44	*Ellagic Acid* **{O=C1OC2=C(C3=C1C=C(O)C(O)=C3OC4=O)C4=CC(O)=C2O}**	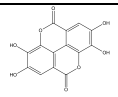	$C_{14}H_6O_8$	300.9988, 300.9979	-	-	-	2.9427	*	-	[22]
24	6.85	*Quercetin* **{OC1=C(C2=CC=C(O)C(O)=C2)OC3=C(C(O)=CC(O)=C3)C1=O}**	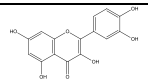	$C_{15}H_{10}O_7$	301.0327, 301.0343	151.1110[$C_7H_3O_4$]	303.0493, 303.0499	-	-5.0948/ -2.1226	*	-	[20]

25	7.20	*Kaempferol 3-glucoside* **{O=c(c(O[C@@H]1O[C@@H]([C@H](C(C1O)O)O)CO)c(c2ccc(O)cc2)o3)c4c3cc(O)cc4O}**	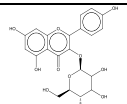	$C_{21}H_{20}O_{11}$	447.0914, 447.0922	284.0324[$C_{15}H_8O_6$], 255.0292[$C_{14}H_7O_5$]	-	-	-1.7617	*	-	[4]
Coumarin group:												
26	5.11	*6,8-dihydroxy-3-methyl-1H-isochromen-1-one* **{OC1=CC(O)=CC2=C1C(OC(C)=C2)=O}**	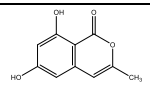	$C_{10}H_8O_4$	191.0349, 191.0339	178.0262[$C_6H_9O_4$], 133.02990[$C_8H_5O_2$]	-	-	5.1385	*	-	[26]
27	7.64	*7-hydroxy-6,8-dimethoxy-2H-chromen-2-one* **{O=C1OC2=C(C=C(OC)C(O)=C2OC)C=C1}**	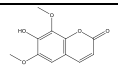	$C_{11}H_{10}O_5$	-	-	223.0594, 223.0601	177.0546[$C_{10}H_9O_3$], 149.0233[$C_8H_5O_3$]	-3.636	*	-	[27]
28	9.18	*7-Hydroxycoumarin* **{O=C1C=CC(C=C[13C](O)=[13CH]2)=[13C]2O1}**	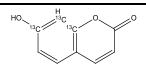	$C_9H_6O_3$	162.0309, 162.0308	133.0277[$C_8H_5O_2$], 121.0279[$C_7H_5O_2$], 177.0330[C_8H_5O]	-	-	-0.6171	*	-	[28]
29	9.56	*(E)-O-Methoxycinnamic acid* **{O=C1OC2=C(C=CC(O)=C2)C=C1}**	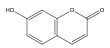	$C_{10}H_{10}O_3$	177.0545, 177.0546	133.0279[$C_8H_5O_2$], 121.0279[$C_7H_5O_2$]	-	-	-0.9153	*	-	MS-Dial
30	11.44	*3,4-dimethoxy 6,8-dihydroxy coumarin* **{O=C1C(OC)=C(OC)C(C=C(O)C=C2O)=C2O1}**	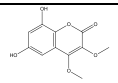	$C_{11}H_{10}O_6$	-	-	239.0541, 239.0544	148.0373[$C_5H_8O_5$]	1.2549	*	-	[25]
Fatty Acids, Tocopherol, and Other Metabolites groups:												
31	11.66	*Ricinoleic acid* **{CCCCCC[C@@H](O)C/C=C\CCCCCCCC(O)=O}**	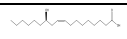	$C_{18}H_{34}O_3$	-	-	299.2477, 299.2478	250.1881[$C_{16}H_{26}O_2$]	0.3341	*	-	[29]
32	11.86	*Kaurene* **{C[C@H]1C[C@@]23CC[C@@H]4C(C)(CCC[C@]4([C@@H]2CC[C@@H]1C3)C)C}**	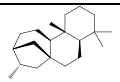	$C_{20}H_{34}$	-	-	275.2736, 275.2733	159.1168[$C_{12}H_{15}$], 133.1012[$C_{10}H_{13}$]	-1.0898	*	-	
33	11.98	*Phaseolin* **{CC1(C)C=Cc2c(ccc3c2O[C@H]2c4cc**	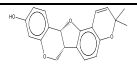	$C_{20}H_{18}O_4$	-	-	323.1264, 323.1278	263.1062[$C_{18}H_{15}O_2$], 157.1222[$C_9H_{18}O_2$], 125.0961[$C_8H_{13}O$]	-4.3707	*	-	

		c(O)cc4OC[C@@H]32)O1}										
34	15.50	*9,10-Dihydroxystearic acid* **{CCCCCCCCCC(O)C(O)CCCCCCCC(O)=O}**	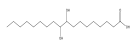	$C_{18}H_{36}O_4$	315.2531, 315.2530	297.2426[$C_{18}H_{33}O_3$]	-	-	0.4988	*	-	
35	22.85	*alpha-Tocopherol* **{Cc1c(O)c(C)c(CC[C@@](CCC[C@@H](CCC[C@@H](CCCC(C)C)C)C)O2)C)c2c1C}**	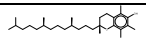	$C_{29}H_{50}O_2$	-	-	431.3871, 431.3884	165.0906[$C_{10}H_{13}O_2$]	-2.8080	*	-	[29]
36	24.04	*Pimelic acid* **{O=C(CCCCCC(O)=O)O}**	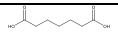	$C_7H_{12}O_4$	-	-	161.0819, 161.0816	111.0552[$C_6H_7O_2$]		*	-	
37	24.39	*Sebacic acid* **{O=C(CCCCCCCCC(O)=O)O}**	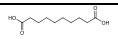	$C_{10}H_{18}O_4$	-	-	203.1288, 203.1278	162.0865[$C_7H_{14}O_4$]	4.8410	*	-	

 # Data between {} = smile of compound, Between [] = chemical formula of fragmentation, (*) detected compound, and (-) not detected compound

3.2. Macroscopic examination

In the present study normal rats that weren't subjected to the carcinogenic DMBA agent or MPA injection, didn't develop any tumours or elevation of the biochemical parameters measured in sera to aid in diagnosis of the disease and follow up of its prognosis throughout the duration of the experiment (16 weeks).

On the other hand, a single dose of 20 mg/kg of DMBA in 1 mL of olive oil by gavage (PO) and repeated injections every other day of MPA by intra muscular (IM) administration for 8 successive weeks, induced breast tumours in the positive control rats of average size 5.53x2.89 mm, some of which showed high vascularity (Figure 1a,b,c, and Figure 3). This carcinogenic effect of DMBA was mentioned by Abdulaziz et al [30] in a previous study, as they stated that admission of DMBA in a dose of 25 mg/kg to rats had induced breast tumours in 100% of the experimental animals used after seven weeks of admission.

While, treatment of rats with total plant extract (10 mg/kg), total alkaloids (5 mg/kg) and recinine (5 mg/kg) showed reduction in the size of tumours and improvement of appearance, denoting efficiency of the tested substances in the prognosis of mammary gland tumours, as the average tumour size of the total plant extract group was 0.72x 0.47mm, average size of tumour of total alkaloids group was 3.15x 1.36 mm and that of recinine group was 4.69x 2.56 mm (Figure 2a, b, c respectively and Figure 3).

3.3. Histopathological finding

Macroscopic examination was followed by histopathologic examination of the suspected excised tumour lesions for confirmation of the diagnosis.

The pathological changes of mammary gland tissue in each group were evaluated by H&E staining. Microscopically, positive group showed destruction of mammary gland architecture with glandular tissue and ductal tissue were occupied by dense populations of malignant cells that are characterized by hyperchromasia and pleomorphism. Some scattered ducts has central necrotic area surrounded by neoplastic epithelial cells; comedocarcinoma; surrounded by poorly detected normal surrounding adipose tissue and occupied by marked fibrosis (Figure 4 A, B,C). Lymph node with metastaic depositis (Figure 4 D).

Group that treated with with recinine showed moderate morphological changes, response showed decrease cellualrity, scattered small foci of malignant cells and increase fibrosis (Figure 5B). After treatment with total alkaloid revealed dilated glands lined with necrotic debris, also there is obvoious fibrosis surrounding glands (Figure 5C). While treatment with total plant showed normal mammary glands surrounded with fibrosis (Figure 5D).

3.4. Biochemical assay of tumour and inflammation markers

Biochemical assay of tumour and inflammatory markers was performed on the pre-mortem collected serum samples, for studying the mechanism of action of the tested carcinogenic and therapeutic substances.

In the current study administration of DMBA together with MPA to rats caused significant elevation of TNFα in the serum of the positive control (untreated) group compared to all groups. Also, DMBA and MPA significantly elevated the levels of PPARα and PI3K in the serum of the positive control (untreated) group compared to all groups, which persisted in treated groups but with variable intensities, with the most marked significant difference in the group treated with total plant extract. The level of STAT3 was significantly high in the positive control group compared to all other groups except the recinine treated group didn't show any significant

difference when compared to the positive control group, and there was marked increase in significance compared to total plant extract group more than the total alkaloids group (Figure 6).

Excitingly, in the present study treatment of rats suffering from breast cancer with total plant extract, total alkaloids and recinine didn't show any significant difference in the levels of TNF α, either between the normal group or between each other, which denotes that the three tested substances possessed anti-inflammatory effects of nearly the same efficacy (Figure 6).

Additionally, the levels of PPARα didn't show any significant difference between all the three treated groups and each other, yet their levels were significantly higher when comparing the three treated groups with the normal group, with the group treated with total plant showing the least significant difference compared to the normal group, which denotes that all the three tested substances exerted their effects via antagonizing PPARα pathway, targeting the molecular mechanism of breast cancer and immune-modulating one its predisposing factors (Figure 6).

Regarding the level of PI3K in serum, only the group treated with the total plant extract didn't show any significant difference when compared to the normal group, while the other two treated groups showed significant increase in the level of PI3K when compared to the normal group, additionally there was significant reduction in the level of PI3K in the group treated with total plant compared to the group treated with recinine, however there wasn't any significant difference in its level between the group treated with the total plant and the group treated with total alkaloids, or between the group treated with total alkaloids and the group treated with recinine (Figure 6).

Also the levels of the STAT3 didn't show any significant difference between all the three treated groups and each other, moreover there wasn't any significant differences between the groups treated with the total plant extract and the total alkaloids on one hand and the normal group on the other hand, only the group treated with recinine showed significant increase compared to the normal group. (Figure 6).

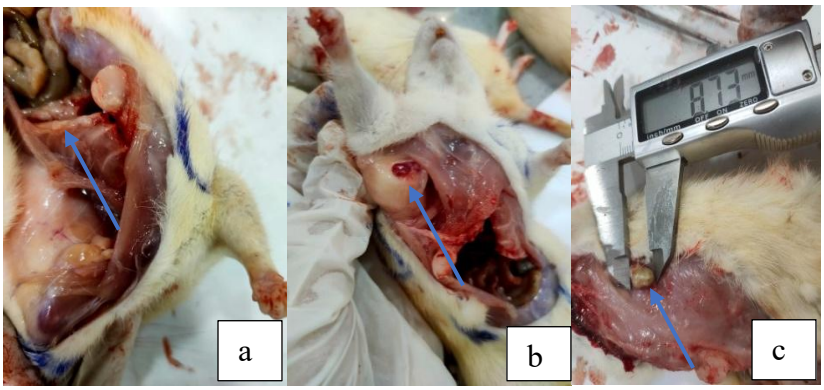

Figure 1: Positive control group given only DMBA and MPA and left without treatment throughout the experiment(a)multilobed tumour, (b)highly vascularized tumour, (c)large tumour

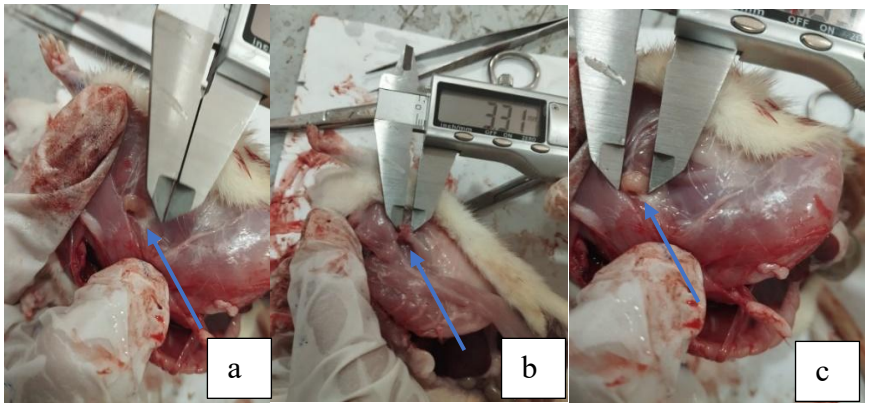

Figure 2: Groups treated with (a)Total plant extract, (b)Total alkaloids and (c)Recinine.

Effect of administration of Total plant, Total alkaloids and Recinine on breast tumour size.

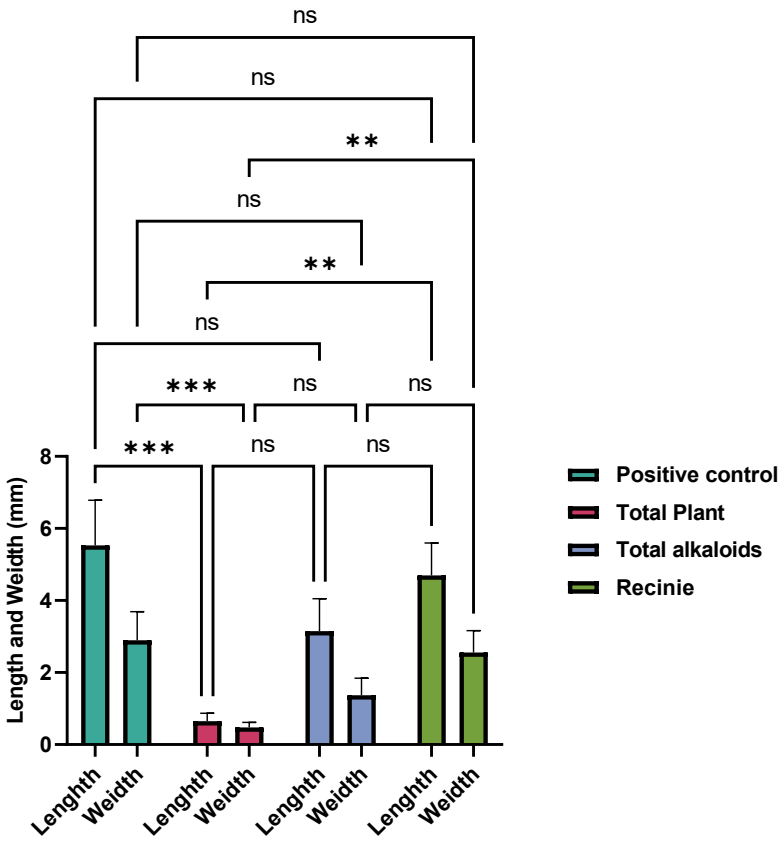

Figure 3: Results of tumour dimensions are expressed as means of sizes in mm± SE, N=5, comparison between means was done by two way analysis of variance (ANOVA), followed by Tukey Kramer's test, P value ≤ 0.05.

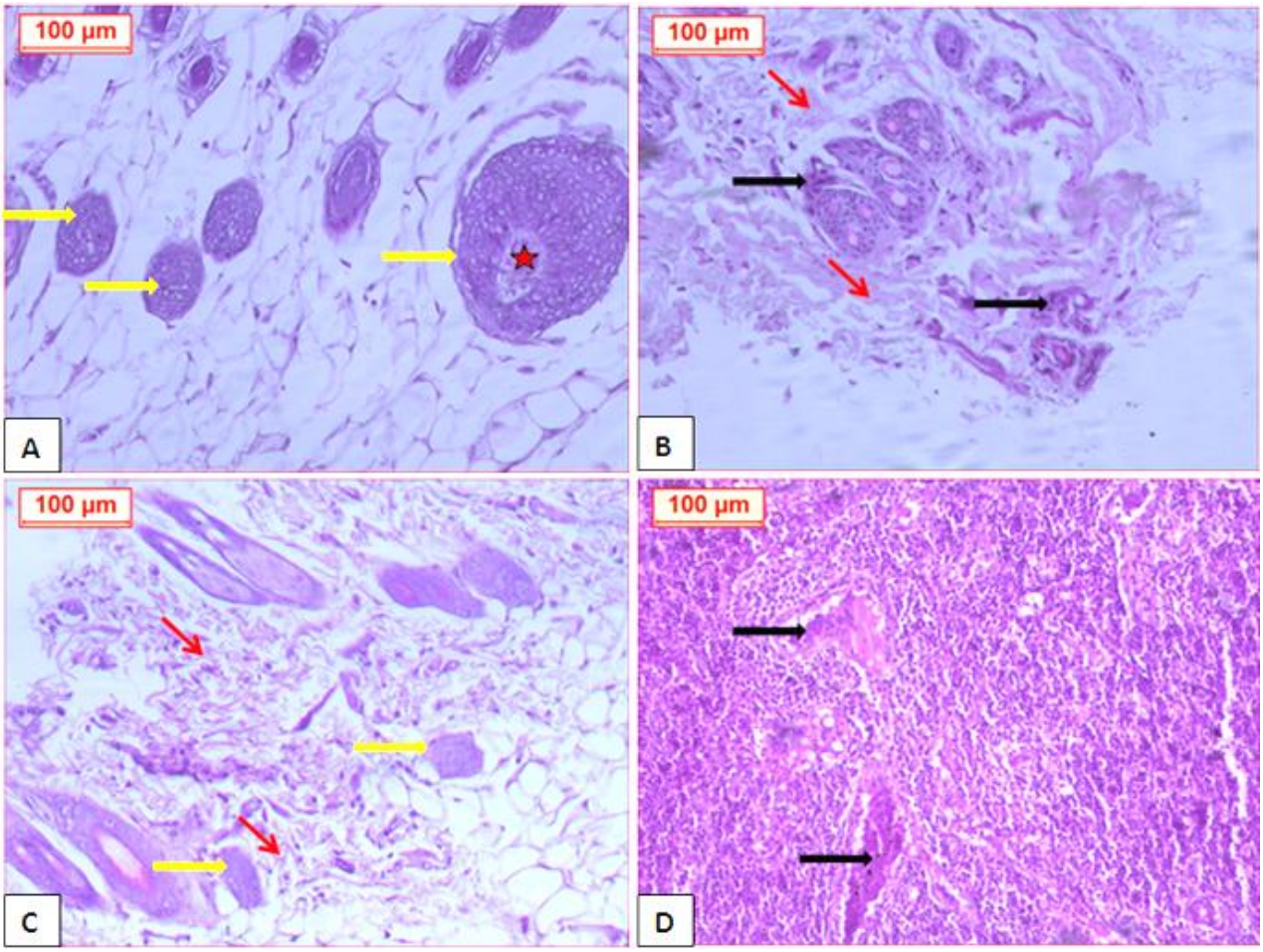

Figure 4: photomicrograph of mammary gland tissue show **A**,**B,C:** Malignant positive group show dilated duct with neoplastic epithelial cells I (yellow arrow), some with central necrosis (star), scattered foci of neoplastic cells (black arrow), surrounded by desmoplastic reaction (red arrow). **D:** Lymph node with metastatic deposits (black arrow) (H&E X200)

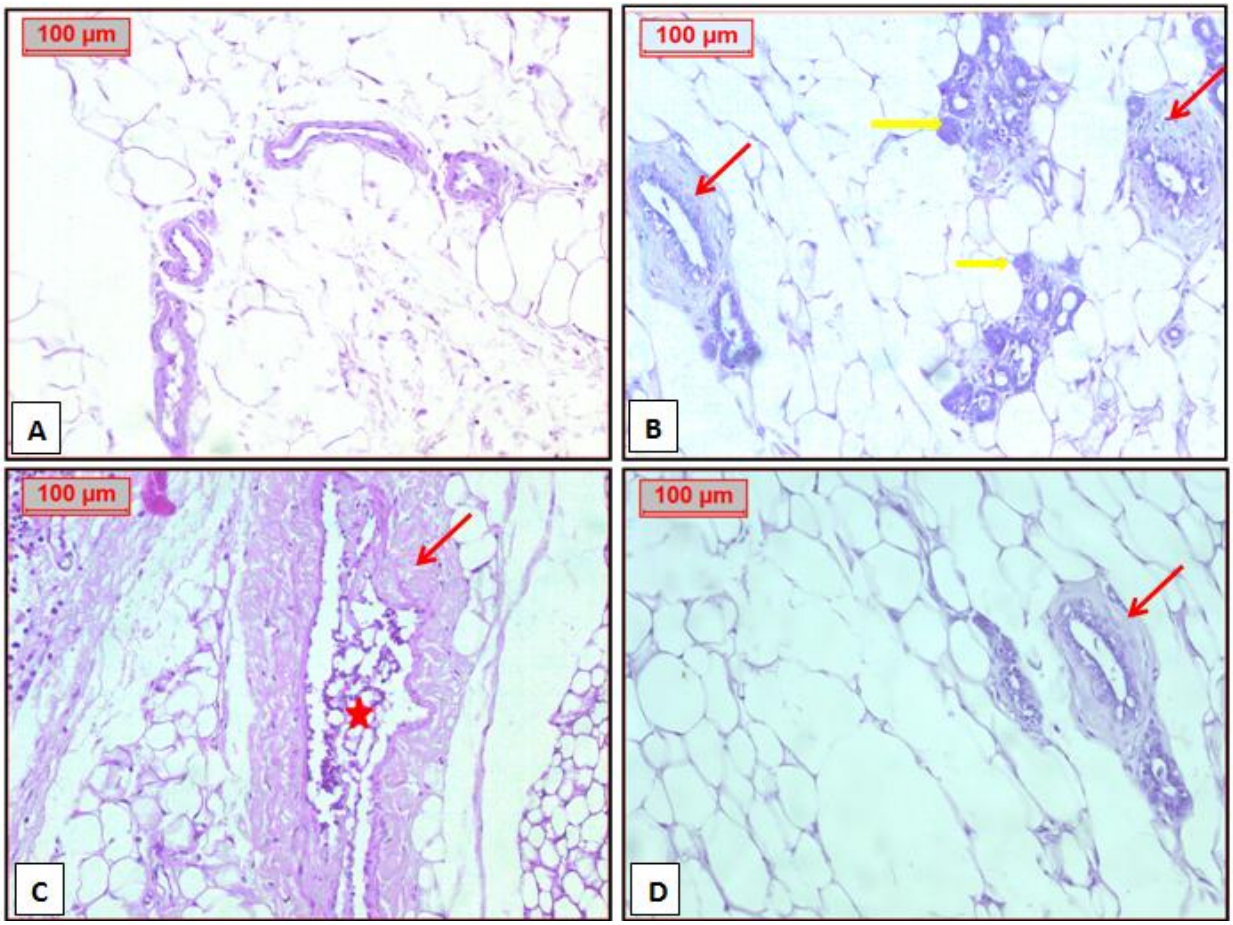

Figure 5: photomicrograph of mammary gland tissue show **A:** normal mammary gland. **B:** recinine treated group showed malignant foci (yellow arrow) and fibosis (red arrow) **C:** total alkaloid treated group showed dilated gland with debris (star) surrounded with fibrosis (red arrow). **D:** total plant extract treated group is similar to normal with fibrosis (red arrow) (H&E X200)

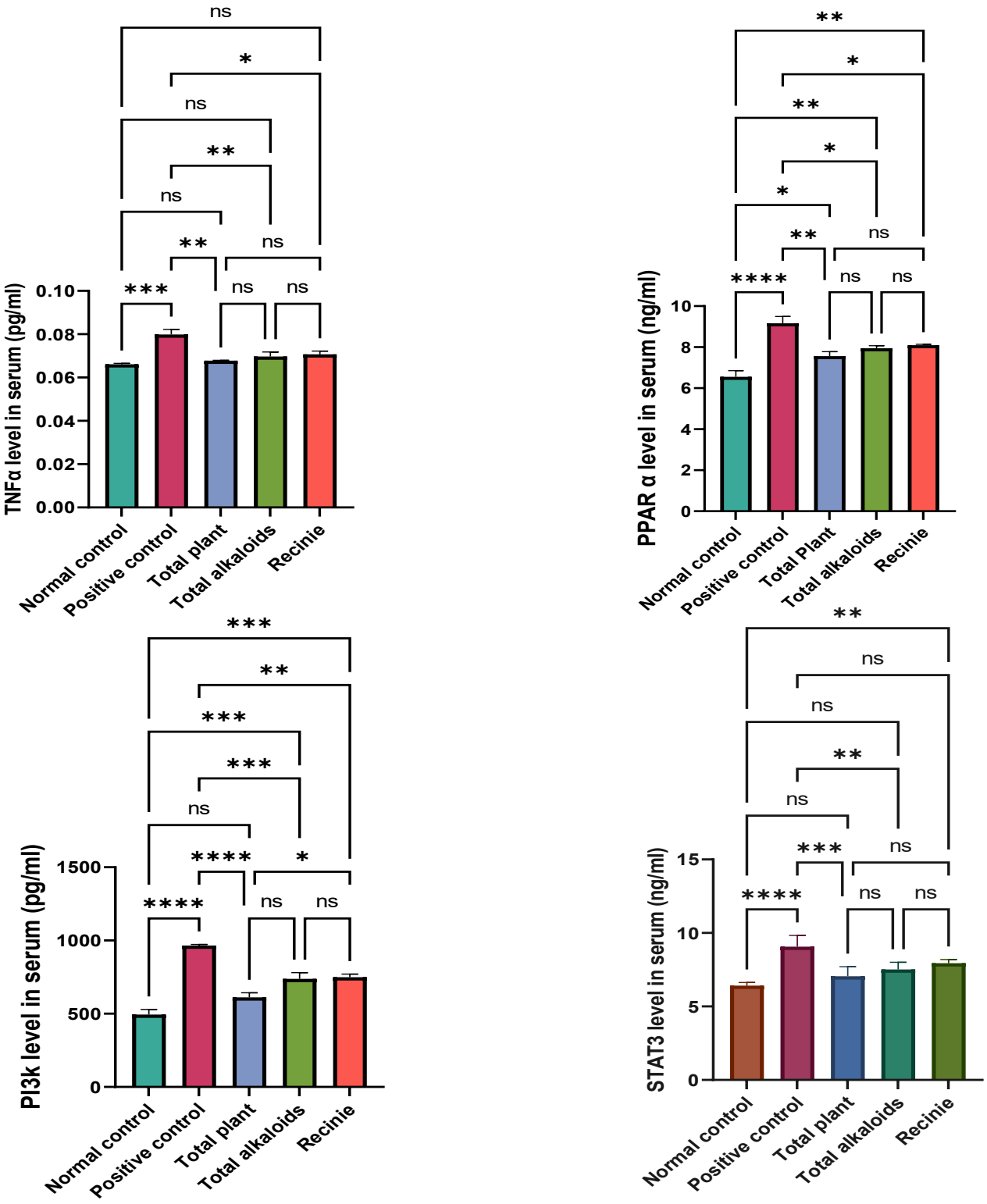

Figure 6: Results of Inflammatory and Tumour markers are expressed as means of levels in sera ± SE, N=5, comparison between means was done by one way analysis of variance (ANOVA), followed by Tukey Kramer's test, P value ≤ 0.001.

3.5. Molecular Modeling

Based on the Autodock Vina docking results presented in the two tables, the plant extract compounds demonstrate notable binding affinities and specific interactions with the target proteins, Peroxisome proliferator-activated receptor gamma (PPARγ) and PI3-K enzyme. For PPARγ (Table 2), the calculated binding energies (S-scores) range from -7.69 to -14.35 kcal/mol, with several ligands exhibiting exceptionally strong binding below -10 kcal/mol (e.g., ligands: 17, 18, 19, 21, 27, 28, 31, 32, and 33). Key amino acid residues involved in hydrogen bonding interactions across multiple ligands include Ser289, Tyr327, Tyr473, and His449, suggesting these are critical anchor points within the PPARγ binding pocket. Notably, some ligands form multiple hydrogen bonds, such as ligand 21, which interacts with Ser289 and His323, Figure 7A. For the PI3-K enzyme (Table 3), the binding energies range from (-6.77 to -14.36) kcal/mol, with the strongest binders including ligands 15, 16, 17, 21, 27, and 28. The predominant interactions involve residues such as Val882, Asp841, Tyr867, Ser806, and Lys833. Ligands 15 and 17, which show high binding affinity (-14.36 and -13.74 kcal/mol, respectively), form hydrogen bonds with Ser806/Lys802 and Glu880, indicating potent and specific binding Figure 7B. A comparative analysis reveals that while both targets show ligands with strong binding energies below (-10) kcal/mol, the PPARγ dataset features a greater number of high-affinity ligands and a more diverse set of interacting residues, including Cys285 and Phe282, which are not observed in the PI3-K interactions. These results suggest that the plant extract contains promising compounds with dual inhibitory potential against both PPARγ and PI3-K, warranting further investigation for their therapeutic applications.

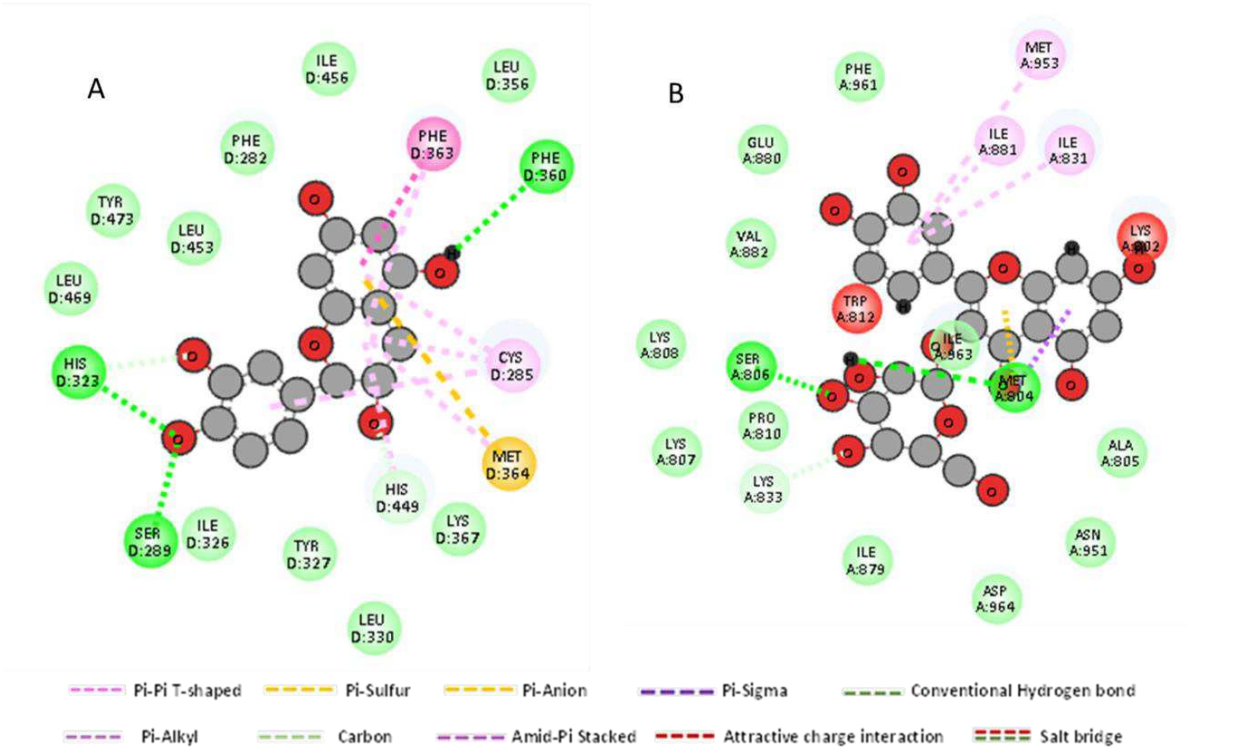

Figure 7: Molecular visualization of quercetin at the catalytic binding sites of Peroxisome proliferator-activated receptor gamma (PPAR γ) protein receptor[A],and. Quercetin 3-O-galactoside at the catalytic binding sites of PI3-K enzyme [B].

Table 2: Summary of Autodock Vina docking results for the plant extract with Peroxisome proliferator-activated receptor gamma (PPAR γ) protein.

ligands	***Hydrogen bonds between atoms of ligands and amino acids of receptor***					**S- score** (binding energy) (kcal/mol)
	ligands Atoms	receptor		Type	Distance (Å)	
		Atoms	Residues			
1,3-dimethylpyridin-2(1H)-one (1)	O8420	O 4818	CYS 285	H-don	2.90	-9.38
1-methylpyridin-2(1H)-one(2)	No Interaction					
4-methoxy-2-oxo-1,2-dihydropyridine-3-carbonitrile(3)	N8437	OG48 94	Ser 289	H-acc	2.88	-10.22
4-(dimethylamino)benzaldehyde(4)	H8421	OH55 04	Tyr 327	H-acc	2.19	-10.57
	O 8429	OH 7886	Tyr 473	H-acc	2.82	
4-methoxy-1-methyl-2-oxo-1,2-dihydropyridine-3-carbonitrile(5)	O8425	NE 7476	His 449	H-acc	2.58	-8.47
1-methyl-2-oxo-1,2-dihydropyridine-3-carbonitrile(6)	N8416	OG48 94	Ser 289	H-acc	2.48	-9.37
4-methoxy-1-methyl-2-oxo-1,2-dihydropyridine-3-carboxylic acid(7)	O8417	ND54 2	His 323	H-acc	2.84	-7.69
	O8417	OH78 86	Tyr 473	H-acc	2.64	
1-methyl-2-oxo-dihydropyridine-3-carbonitrile(8)	No Interaction					
1-methyl-6-oxo-1,6-dihydropyridine-3-carbonitrile(9)	O 8416	OH 5504	TYR 327	H-acc	2.73	-9.32
	N 8418	OH 7886	TYR 473	H-acc	3.31	
1-methyl-9H-pyrido[3,4-b]indole(10)	N 8419	OG 4894	SER 289	H-acc	3.32	-8.227
methyl 5-(3-cyano-2-oxo-1,2-dihydropyridin-4-yl)pentanoate(11)	N 8419	NE 7476	HIS 449	H-acc	2.89	-8.321
methyl 5-(2-oxo-1,2-	O 8418	OG	SER	H-don	2.72	-10.7

dihydropyridin-4-yl)pentanoate(12)		4894	289			
1-methyl-4-((4-methylpentyl)oxy)-5,6-dihydropyridin-2(1H)-one(13)	O 8413	OH 7886	TYR 473	H-don	2.50	-8.178
methyl 5-(3-cyano-1-methyl-2-oxo-1,2-dihydropyridin-4-yl)pentanoate(14)	No interaction					
Quercetin 3-O-galactoside(15)	No interaction					
Gallic acid(16)	No interaction					
Ellagic Acid(17)	O 8468	O4817	Gly 284	H-don	1.71	-14.02
Gentisic acid(18)	H 8421	O 4774	PHE282	H-don	3.25	-12.50
Quercetin 3-rutinoside(19)	O 8409	OG 4894	SER 289	H-don	3.06	-13.9
Epicatechin(20)	No interaction					
Quercetin(21)	O 8433	OG 4894	SER 289	H-don	2.46	-14.35
	O 8433	OG 4894	SER 289	H-acc	2.46	
	O 8433	ND 5426	HIS 323	H-acc	2.74	
7-hydroxy-2H-chromen-2-one(22)	No interaction					
Methylgallate(23)	O 8420	N 5722	SER 342	H-acc	3.17	-8.90
Kaempferol 3-glucoside(24)	No interaction					
7-Hydroxycoumarin(25)	O 8454	OH 5504	TYR 327	H-don	2.51	-10.38
	O 8454	OH 5504	TYR 327	H-acc	2.51	
Ricinoleic acid(26)	No interaction					
Phaseolin(27)	O 8424	OG 5731	SER 342	H-don	2.24	-12.05
	O 8428	OG 5731	SER 342	H-don	2.71	
Indole-3-acetic acid(28)	O 8470	OH 5504	TYR 327	H-don	1.88	-11.70
	O 8474	NE 7476	HIS 449	H-don		
Kaempferol 3-rutinoside(29)	H 8407	O 4818	CYS 285	H-don	2.16	-9.31

9,10-Dihydroxystearic acid(30)	No interaction					
6, 7-dihydroxy 8-methoxy coumarin(31)	H 8418	O 4774	PHE 282	H-don	1.97	-12.61
	H 8420	OE 4837	GLN 286	H-don	3.00	
3,4-dimethoxy 6,8-dihydroxy coumarin(32)	O 8460	OH 5504	TYR 327	H-don	3.00	-10.83
	O 8458	NE 7476	HIS 449	H-don	2.6	
7-hydroxy-6,8-dimethoxy-2H-chromen-2-one(33)	O 8423	OG 4894	SER 289	H-don	2.94	-11.99
	O 8418	OG 4894	SER 289	H-acc	2.61	

Table 3: Summary of Autodock Vina docking results for the plant extract with PI3-K enzyme protein.

ligands	***Hydrogen bonds between atoms of ligands and amino acids of receptor***					**S- score** (binding energy) (kcal/mol)
	ligands Atoms	receptor		Type	Distance (Å)	
		Atoms	Residues			
1,3-dimethylpyridin-2(1H)-one(1)	O 13773	OD 9919	ASP 841	H-don	2.62	-9.43
	O 13773	OH 10365	TYR 867	H-don	2.28	
1-methylpyridin-2(1H)-one(2)	No interaction					
4-methoxy-2-oxo-1,2-dihydropyridine-3-carbonitrile(3)	No interaction					
4-(dimethylamino)benzaldehyde(4)	O 13772	O 10571	VAL 882	H-don	2.96	-8.57
	N 13764	N 10566	VAL 882	H-acc	2.19	
4-methoxy-1-methyl-2-oxo-1,2-dihydropyridine-3-carbonitrile(5)	O 13778	N 10566	VAL 882	H-acc	2.59	-8.82
1-methyl-2-oxo-1,2-dihydropyridine-3-carbonitrile(6)	N 13769	NZ 9796	LYS 833	H-acc	2.46	-8.97
4-methoxy-1-methyl-2-oxo-1,2-dihydropyridine-3-	No interaction					

carboxylic acid(7)						
1-methyl-2-oxo-dihydropyridine-3-carbonitrile(8)	O13771	N10566	Val882	H-acc	2.83	-6.77
1-methyl-6-oxo-1,6-dihydropyridine-3-carbonitrile (9)	N 13771	NZ 9796	LYS 833	H-acc	2.49	-7.62
1-methyl-9H-pyrido[3,4-b]indole(10)	O 13770	N 10566	VAL 882	H-acc	2.40	-7.54
methyl 5-(3-cyano-2-oxo-1,2-dihydropyridin-4-yl)pentanoate(11)	N 13772	N 10566	VAL 882	H-acc	2.50	-7.43
methyl 5-(2-oxo-1,2-dihydropyridin-4-yl)pentanoate(12)	No interaction					
1-methyl-4-((4-methylpentyl)oxy)-5,6-dihydropyridin-2(1H)-one(13)	N 13761	OH 10365	TYR 867	H-don	3.03	-8.39
	O 13766	OH 10365	TYR 867	H-don	2.87	
methyl 5-(3-cyano-1-methyl-2-oxo-1,2-dihydropyridin-4-yl)pentanoate(14)	No interaction					
Quercetin 3-O-galactoside(15)	O 13777	OG 9350	SER 806	H-don	2.37	14.36-
	O 13802	NZ 9294	LYS 802	H-acc	1.73	
Gallic acid(16)	O 13770	OG 9350	SER 806	H-don	2.97	-13.37
Ellagic Acid(17)	H 13797	O 10537	GLU 880	H-don	2.17	-13.74
Gentisic acid(18)	H 13763	OD 11846	ASP 964	H-don	1.69	-10.21
Quercetin 3-rutinoside(19)	O 13777	O 10571	VAL 882	H-don	2.17	-12.79
Epicatechin(20)	O 13757	OD 9919	ASP 841	H-don	2.74	-9.81
Quercetin(21)	O 13790	N 11836	ASP 964	H-acc	2.77	-12.81
7-hydroxy-2H-chromen-2-one(22)	O 13774	N 10566	VAL 882	H-acc	3.19	-10.00
Methylgallate(23)	No interaction					

Kaempferol 3-glucoside(24)	H 13774	O 10537	GLU 880	H-don	2.44	-8.47
7-Hydroxycoumarin(25)	H 13809	OD 9919	ASP 841	H-don	3.74	-10.08
Ricinoleic acid(26)	O 13787	OG 9350	SER 806	H-don	2.32	-10.86
Phaseolin(27)	O 13801	N 9331	ALA 805	H-acc	2.57	-13.02
Indole-3-acetic acid(28)	O 13784	OG 9350	SER 806	H-don	2.65	-12.86
Kaempferol 3-rutinoside(29)	O 13757	O 10571	VAL 882	H-don	2.87	-10.30
9,10-Dihydroxystearic acid(30)	O 13776	NZ 9796	LYS 833	H-acc	2.80	-9.58
	O 13778	NZ 9796	LYS 833	H-acc	2.89	`
6, 7-dihydroxy 8-methoxy coumarin(31)	O 13808	O 10571	VAL 882	H-don	2.79	-10.48
3,4-dimethoxy 6,8-dihydroxy coumarin(32)	H 55	O 10609	GLU 880	H-don	2.92	-10.20
7-hydroxy-6,8-dimethoxy-2H-chromen-2-one(33)	No interaction					

4. Discussion

Comprehensive LC–MS/MS profiling of *Ricinus communis* revealed 37 metabolites belonging to pyridone alkaloids, flavonoids, phenolic acids, coumarins, fatty acids, and diterpenes, confirming the remarkable chemical diversity of the extract. Previous phytochemical investigations have similarly identified ricinine alkaloids, flavonoids, and phenolic constituents as major bioactive metabolites in *R. communis*, supporting its reported antioxidant, anti-inflammatory, and anticancer properties[31]. In agreement with earlier reports demonstrating that *R. communis* fruit extract suppresses breast cancer cell proliferation, migration, invasion, and tumour progression *in vivo*, the present findings further highlight the chemopreventive potential of its leaf metabolites and alkaloid-rich fraction[32]. Importantly, three putative pyridone alkaloid derivatives were tentatively identified and investigated for anticancer relevance for the first time, substantially expanding the phytochemical profile of the plant. Considering the established contribution of natural alkaloids to clinically used anticancer drugs such as vincristine, vinblastine, and irinotecan, these metabolites may represent promising chemopreventive chemotypes[33]. Moreover, the superior biological activity observed for the total extract compared with isolated ricinine highlights the importance of phytochemical synergy in mediating the observed anti-inflammatory and anticancer effects. ***Total alkaloids fraction vs. Total extract composition:*** The total alkaloids fraction was highly enriched in nitrogen containing metabolites, particularly pyridone-type alkaloids. Ricinine, the principal alkaloid marker of *R. communis*, was the most abundant compound, consistent with its reported occurrence across multiple plant tissues. In addition to ricinine, several substituted 2-pyridone and dihydropyridone derivatives were detected. Many of these compounds share core structural features with previously described pyridone alkaloids that have insecticidal and antimicrobial

activities [34] . In contrast, the total extract exhibited a broader chemical diversity, containing not only pyridone alkaloids but also significant quantities of phenolic acids (e.g., gallic, gentisic, ellagic acids), flavonoids and their glycosides (e.g., quercetin, epicatechin, kaempferol derivatives), fatty acids including ricinoleic acid, and other lipid-related metabolites. Such a diverse metabolite profile aligns with literature reports on the phytochemical complexity of *R. communis*, which describe the presence of multiple classes of bioactive compounds in leaves, seeds, and roots[31]. The total extract therefore reflects the holistic phytochemical makeup of *R. communis*, whereas the total alkaloids fraction represents a more focused subset dominated by basic nitrogenous compounds. This distinction is important for interpreting biological activity, as the total extract's composite profile allows for multi-target interactions, while the alkaloid fraction isolates the contributions of specific nitrogenous constituents.

New Pyridone Alkaloids and Structural Significance: Among the detected alkaloids, three pyridone derivatives methyl 5-(2-oxo-1,2-dihydropyridin-4-yl)pentanoate, methyl 5-(3-cyano-2-oxo-1,2-dihydropyridin-4-yl)pentanoate, and 1-methyl-2-oxo-dihydropyridine-3-carbonitrile are reported here for the first time in *R. communis*. These compounds expand the known structural variation of plant pyridone derivatives by incorporating aliphatic ester side chains and nitrile substituents, features more commonly associated with synthetic medicinal analogues than with botanical extracts. Nitrile functional groups, in particular, are recognized for enhancing metabolic stability and target affinity in drug design, suggesting that such compounds merit further pharmacological evaluation. The pyridone core itself is a well-recognized pharmacophore in medicinal chemistry, with 2-pyridone and 4-hydroxy-2-pyridone derivatives documented to exhibit anticancer, antimicrobial, and anti-inflammatory effects in various studies. While most such research has centered on synthetic libraries or microbial natural products, the presence of structurally diverse pyridones in *R. communis* broadens the scope of plant-derived pyridone chemistry [3]. High-resolution MS/MS fragmentation provided strong structural support for the identified metabolites. Observed precursor ions exhibited excellent mass accuracy ($\Delta < 2$ ppm), and fragmentation paths were characterized by neutral losses of CN, CO, CH_3, and ester side chains, consistent with typical behaviors for substituted pyridones and lactam systems. These fragmentation patterns align with those reported for alkaloids in natural product studies, reinforcing confidence in metabolite annotations.

The detection of phenolic acids and flavonoids, such as gallic acid, quercetin, and epicatechin, corroborates previous studies documenting high antioxidant capacity in *R. communis* extracts, which have been linked to radical scavenging and anti-inflammatory effects [35]. Phenolic compounds are widely recognized for modulating oxidative stress and inflammatory pathways, processes that frequently intersect with tumorigenesis. Their presence alongside pyridone alkaloids in the total extract suggests potential synergistic actions, wherein antioxidant and anti-inflammatory metabolites may mitigate pro-oxidative and proliferative signals. While direct anticancer bioactivity of natural ricinine and related alkaloids in mammalian systems has been less extensively characterized, isolated pyridone and heterocyclic derivatives have been shown to modulate cell signaling pathways relevant to proliferation and survival. Additionally, ricinine itself has been implicated in signaling modulation through pathways such as Wnt/β-catenin, demonstrating effects on cellular signaling components in experimental models. The combined presence of alkaloids, phenolics, and flavonoids in the total extract enhances the potential for multi-target modulation of inflammatory and proliferative pathways such as PI3K/AKT and STAT3, which are central to breast cancer progression [36].

The significant elevation of TNFα in the serum of the positive control (untreated) group compared to all other groups in the current study, due to administration of DMBA together with MPA to rats, was in agreement with the former study of Abdulaziz et al [30].

Previous studies have postulated that lipid abnormalities in the tumor micro-environment were confirmed to be present in breast cancer. Peroxisome proliferator-activated receptor alpha (PPARα) is a ligand-activated transcriptional factor and is one of the nuclear receptor family. PPARα is a key regulator of lipid metabolism and controls the expression of genes related to fatty acid balance, by controlling genes involved in the lipogenic pathway, oxidative as well as activation processes of fatty acids, in addition to exogenous fatty acids uptake. PPARα also contributes to the control of the tumor microenvironment by exhibiting anti-inflammatory activity [37], and by suppression of angiogenesis, through immunomodulation of PI3 /AKT/ mTOR pathway [38]. It had been postulated by Wang et al [39], that via uncoupled fatty acid oxidation and synergistic adipose triglyceride (TG) lipase–dependent (ATGL-dependent) lipolysis, the peri-tumoral fat cells facilitated tumour invasion to the breast. PPARα activation causes ATGL consequences such as autophagy, oxidative damage, and inflammation [40].

When comparing breast cancer tissue and cell lines to healthy controls, PPARα expression is frequently markedly elevated. This enhanced expression, which is mediated by activation through arachidonic acid (AA), is linked to higher proliferation in some breast cancer cells. The overall effect of PPARα can vary depending on the particular breast cancer cell line and other circumstances, and its function is complicated because PPARα agonists have also been demonstrated to decrease proliferation in other cell types. Significantly, PPARα can suppress tumor angiogenesis by downregulating cytochrome P2C44 (CYP2C44). The cytochrome P450 epoxygenase pathway transforms AA into epoxyeicosatrienoic acids (EETs), which are proangiogenic lipid metabolites positively linked to the progression of cancer. EETs stimulate angiogenesis by activating p38, phosphatidylinositol 3-kinase (PI3K), and extracellular signal-regulated protein kinase (ERK) [38].

One of the most crucial pathways that enhance tumour proliferation in breast cancer cases is the phosphoinositide 3-kinase (PI3K) pathway. Alternations in the PI3K/AKT pathway, may encourage the disturbance of the delicate redox, proapoptotic, and antiapoptotic balance, which results in dysregulated cell proliferation and apoptosis avoidance [41]. Modifying small molecules inhibitors that target this pathway has been the aim of therapists involved in compacting breast cancer; there is a rapid rate of progression in that field of studies for the sake of breast cancer patients suffering multidrug resistance [42].

Another important factor involved in breast cancer development is signal transducer and activator of transcription 3 (STAT3), which increases in a drastic way in severe cases of breast cancer. STAT3 regulates genes concerned with cancer chemo-resistance, metastasis, and proliferation. However, its activity can be changed by factors that modulate its interaction with DNA and proteins influencing its transcriptional activity [43].

The highest therapeutic efficacy observed throughout the experiment was achieved by the total plant extract, followed by the total alkaloid fraction, and then recinine compound. The macroscopic findings were consistent with the histopathological results, confirming significant improvement in tumor architecture in treated groups. Furthermore, the assessed biochemical parameters provided mechanistic insight into the potential pathways underlying the anticancer effects of the three tested therapeutic agents in breast cancer management.

The investigated treatments exerted their effects primarily through immunomodulatory mechanisms, effectively controlling inflammatory aggravation, as evidenced by normalization of

tumor necrosis factor-alpha (TNF-α) levels [44]. Chronic inflammation is well recognized as a driving force in breast cancer progression through activation of proliferative and survival signaling cascades[45]. This effect was associated with modulation of peroxisome proliferator-activated receptors (PPARs), particularly PPARγ, a nuclear receptor known to regulate lipid metabolism, inflammation, and tumorigenesis[46]. Antagonistic or modulatory interaction with ligand-activated PPAR signaling may subsequently inhibit the phosphoinositide 3-kinase (PI3K)/Akt pathway, one of the most frequently dysregulated pathways in breast cancer[47], together with suppression of signal transducer and activator of transcription 3 (STAT3), a key mediator of inflammation-driven oncogenesis [48]. The coordinated inhibition of TNF-α, PI3K/Akt, and STAT3 suggests disruption of tumor proliferation, survival signaling, and inflammatory cascades [48].

Molecular docking analysis further validated the chemopreventive potential of *Ricinus communis* and its derivatives, demonstrating strong predicted interactions between extract constituents and key molecular targets implicated in breast cancer progression. For PPARγ, AutoDock Vina results revealed strong binding affinities, with several ligands forming hydrogen bonds with critical amino acid residues within the ligand-binding domain. Previous structural studies have demonstrated that residues such as Ser289, Tyr327, Tyr473, His323, and His449 are essential for stabilizing ligand–receptor interactions and modulating receptor activation [49]. The observed multi-residue engagement suggests potential modulation of PPARγ transcriptional activity, which has been associated with anti-proliferative and pro-differentiation effects in breast cancer models [46]. Similarly, docking against PI3K showed strong predicted binding to residues known to be critical for enzymatic activity. The PI3K/Akt pathway plays a central role in regulating cell growth, metabolism, and resistance to apoptosis in breast cancer [47]. Dual targeting of both PPARγ and PI3K may therefore result in synergistic suppression of tumor proliferation and survival signaling, enhancing the overall therapeutic effect [47]. The chemopreventive activity of the plant extract can be attributed to its rich composition of bioactive metabolites, including flavonoids, phenolic compounds, and other secondary metabolites. Phytochemicals are widely reported to exert anticancer effects through multitarget mechanisms, including antioxidant, anti-inflammatory, and pro-apoptotic activities [50]. Antioxidant constituents reduce ROS, thereby limiting oxidative DNA damage and tumor initiation [51]. Additionally, several plant-derived compounds inhibit proliferative pathways such as Ras/MAPK [52], regulate cell-cycle progression through activation of tumor suppressors p53 and p21 [53], and induce apoptosis via modulation of the PI3K/PTEN axis and activation of caspase-dependent pathways [54] (Figure 8).

Furthermore, plant metabolites may suppress invasion and metastasis by reducing extracellular matrix degradation and downregulating migration-associated markers such as urokinase-type plasminogen activator receptor (uPAR), which is strongly implicated in breast cancer metastasis [55]. The combined multitarget actions of these phytochemicals explain the observed reduction in tumor growth, restoration of biochemical parameters, and improvement in histopathological features in treated groups. Overall, the total plant extract of *Ricinus communis* demonstrates significant chemopreventive and therapeutic potential by regulating inflammatory mediators, proliferation signaling, apoptosis, cell-cycle control, and metastatic pathways in breast cancer.

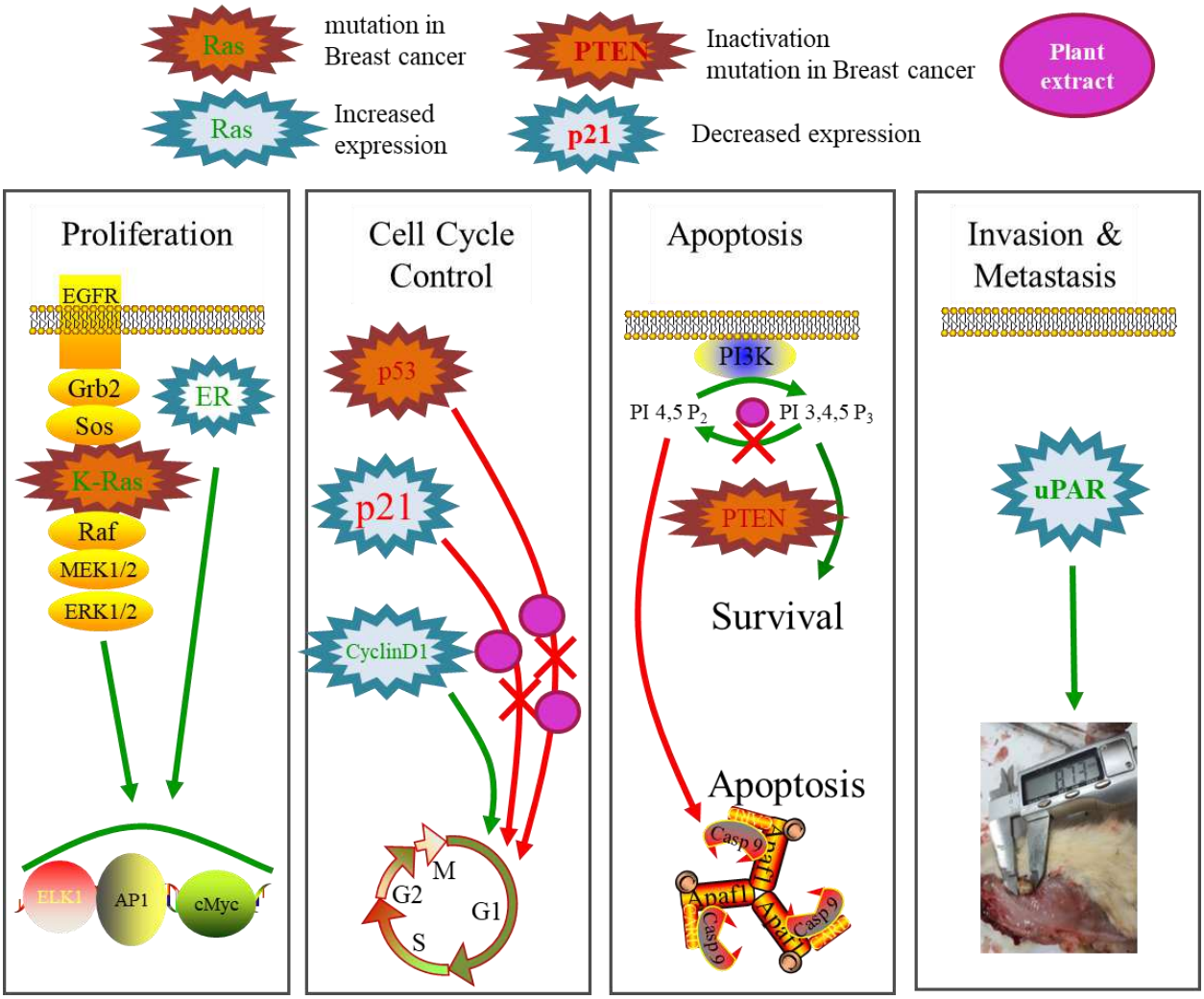

Figure 8: Proposed mechanism of anticancer activity of plant-derived metabolites via regulation of proliferation, apoptosis, and metastatic pathways.

The comparative analysis of both targets indicates that while strong binders exist for both PPARγ and PI3-K, the total plant extract contains a broader array of high-affinity compounds**,** allowing simultaneous modulation of multiple signaling pathways. This multi-target engagement likely explains why the total extract demonstrated superior chemopreventive and immunomodulatory effects *in vivo*, compared to individual alkaloids such as recinine. In essence, the combination of compounds in the total extract provides a synergistic effect, enhancing both efficacy and selectivity, and highlighting the value of natural product mixtures over isolated constituents for therapeutic applications. These docking findings align well with the *in vivo* results, where the total plant extract produced the most pronounced reductions in tumor size, improved mammary gland morphology, and modulation of TNFα, PPARα, PI3K, and STAT3 pathways. Together, these results support the development of *Ricinus communis* total extract as a promising multi-target natural chemopreventive agent against breast cancer.

5. Conclusions

This study offered new products that targeted the molecular mechanisms of breast cancer and immune-modulated some factors that contributed to its development, with the highest effect observed for the total extract, followed by total alkaloids and then ricinine. However, more preclinical trials, especially those involving larger animals, followed by clinical trials, are required for better evaluation of their precise role in cancer management. This could be complemented by the development of refined drug delivery systems that enhance the compliance and therapeutic efficacy of the three substances tested in the current study. In summary, fractionation of *R. communis* extract into total alkaloids and total extract reveals distinct metabolite distributions, with the alkaloid fraction enriched in pyridone derivatives and the total extract encompassing a broader spectrum of bioactive classes. The discovery of novel pyridone alkaloids expands the phytochemical diversity of this species and suggests avenues for future biological evaluation. The presence of complementary bioactive constituents in the total extract supports its multifaceted therapeutic potential, aligning with ethnopharmacological uses of the plant and highlighting its relevance in anti-inflammatory and anticancer research.

Declarations

Ethics approval: The study was conducted in accordance with current ethical principles, including strict adherence to standards related to plagiarism, research misconduct, data fabrication or falsification, duplicate publication, and redundancy. All experimental procedures involving animals followed the National Guide for the Care and Use of Laboratory Animals (NIH publication 86-23, revised 1985) as well as the relevant guidelines of the Academy of Sciences. Ethical clearance was granted by the Institutional Animal Ethics Committee (IAEC) in compliance with national animal welfare regulations. The study was approved by the Research Centre Ethics Committee under approval number (0-8-3).

Clinical trial number: not applicable.

.

Consent for Publication: All authors of the current work agree to have this article published in your journal.

Data Availability Statement: The datasets generated and/or analysed during the current study are available from the corresponding author upon reasonable request. Supplementary data associated with this article, including LC–MS/MS metabolite annotations and NMR spectral data, are provided in the Supplementary Information file.

Competing interests: The authors declare that they have no conflicts of interest related to this work.

Funding: This work was supported by the National Research Centre (NRC), Egypt, under Project No. 13010142, *"Study of active compounds from medicinal plants and their impact on the development of cancer services, especially aromatase inhibitors in breast cancer treatment"* (2022–2025), under the supervision of Dr. Ahmed A. El-Rashedy (PI). Open access funding was provided by the Science, Technology & Innovation Funding Authority (STDF) in cooperation with the Egyptian Knowledge Bank (EKB). No additional research funding was received. The

authors declare that the phytochemical and pharmacological investigations were conducted through self-funding.

Author Contributions: ***MAM*** she contributed to conceptualization, methodology, plant extraction, and biochemistry analysis, and was responsible for methodology, investigation, data curation, as well as drafting, reviewing, and editing the manuscript. ***BMMI*** she contributed to conceptualization, methodology, investigation, data curation, and drafting, reviewing, and editing of the in vivo pharmacological study. ***NEI*** she contributed to investigation, formal analysis, data curation. ***MES*** contributed to conceptualization, investigation, formal analysis, histopathological methodology, formal analysis, and writing. ***AAE*** he contributed to conceptualization, methodology, investigation, data curation, as well as drafting, reviewing, and editing the manuscript. All authors have revised the final document and agree to its publication.

Acknowledgments: The authors thank the National Research Centre (NRC) for providing the necessary facilities and technical support for this work. We gratefully acknowledge Prof. Dr. Hab. Piotr Kachlicki, Institute of Plant Genetics, Polish Academy of Sciences (PAS), Poznań, for his support with UPLC/HRMS analysis.

6. References

1. Jobre, B. and B. Avezbakiyev, *Breast cancer: Global patterns of incidence, mortality, and trends.* Journal of Clinical Oncology, 2023. **41**(16): p. 10528-10528.
2. Cha, H.K., et al., *Discovery of proteins responsible for resistance to three chemotherapy drugs in breast cancer cells using proteomics and bioinformatics analysis.* Molecules, 2022. **27**(6): p. 1762.
3. Abomughaid, M.M., et al., *A phytochemical and pharmacological review of Ricinus communis L.* Discover Applied Sciences, 2024. **6**(6): p. 315.
4. Kang, S.S., et al., *Alkaloids and flavonoids from Ricinus communis.* Journal of natural products, 1985. **48**(1): p. 155-156.
5. Raza, H., et al., *Ricinus Communis: Nutritional Importance, Health Benefits, and Industrial Applications.* eFood, 2026. **7**(1): p. e70117.
6. Mohammed, M.A., et al., *Synergistic effect of Silver and ZnO nanoparticles green synthesized by Vitis vinifera stem extract with Ampicillin against some pathogenic microbes.* Egyptian Journal of Chemistry, 2022. **65**(5): p. 697-709.
7. Mohammed, M.A., et al., *Comprehensive Tools of Alkaloid/Volatile Compounds–Metabolomics and DNA Profiles: Bioassay-Role-Guided Differentiation Process of Six Annona sp. Grown in Egypt as Anticancer Therapy.* Pharmaceuticals, 2024. **17**(1): p. 103.
8. Barros, A.C.S., et al., *Induction of experimental mammary carcinogenesis in rats with 7, 12-dimethylbenz (a) anthracene.* Revista do Hospital das Clínicas, 2004. **59**: p. 257-261.
9. Xia, H.-J., et al., *PTEN/PIK3CA genes are frequently mutated in spontaneous and medroxyprogesterone acetate-accelerated 7, 12-dimethylbenz (a) anthracene-induced mammary tumours of tree shrews.* European journal of cancer, 2014. **50**(18): p. 3230-3242.
10. Badami, S., et al., *Antitumor activity of total alkaloid fraction of Solanum pseudocapsicum leaves.* Phytotherapy Research: An International Journal Devoted to

Pharmacological and Toxicological Evaluation of Natural Product Derivatives, 2003. **17**(9): p. 1001-1004.
11. Kamel, A.A., A. Taye, and M. Khalifa, *Treatment with NaHS reduces systolic blood pressure and ameliorates oxidative stress in DOCA-Salt hypertensive rats.* Journal of Advanced Biomedical and Pharmaceutical Sciences, 2019. **2**(1): p. 7-11.
12. Trott, O. and A.J. Olson, *AutoDock Vina: improving the speed and accuracy of docking with a new scoring function, efficient optimization, and multithreading.* Journal of computational chemistry, 2010. **31**(2): p. 455-461.
13. Gampe, R.T., et al., *Asymmetry in the PPARγ/RXRα crystal structure reveals the molecular basis of heterodimerization among nuclear receptors.* Molecular cell, 2000. **5**(3): p. 545-555.
14. Knight, Z.A., et al., *A pharmacological map of the PI3-K family defines a role for p110α in insulin signaling.* Cell, 2006. **125**(4): p. 733-747.
15. Berman, H.M., et al., *The protein data bank.* Biological Crystallography, 2002. **58**(6): p. 899-907.
16. Zeleke, D., et al., *Synthesis and antibacterial, antioxidant, and molecular docking analysis of some novel quinoline derivatives.* Journal of Chemistry, 2020. **2020**(1): p. 1324096.
17. Rumape, O., et al., *Isolating antifidan compounds of kepyar castor seeds (Ricinus communis L.) to the beetle Epilachna varivestis mulsant,(Coleoptera: Coccinelidae).* Int. J. ChemTech Res, 2014. **6**: p. 3784-3790.
18. Tan, Y.-N., et al., *Pyridone alkaloids from the leaves of Ricinus communis and their inhibitory effect against protein tyrosine phosphatase 1B.* Chemistry of Natural Compounds, 2019. **55**(2): p. 395-397.
19. Villemin, D., et al., *An Convenient Synthesis of Ricinine and Its Analogues.* Chemistry Proceedings, 2021. **8**(1): p. 74.
20. Ribeiro, P.R., R.D. de Castro, and L.G. Fernandez, *Chemical constituents of the oilseed crop Ricinus communis and their pharmacological activities: A review.* Industrial Crops and Products, 2016. **91**: p. 358-376.
21. Allen, J. and D. Baker, *Free tryptophan and indole-3-acetic acid levels in the leaves and vascular pathways of Ricinus communis L.* Planta, 1980. **148**(1): p. 69-74.
22. Singh, P.P. and S. Chauhan, *Activity guided isolation of antioxidants from the leaves of Ricinus communis L.* Food chemistry, 2009. **114**(3): p. 1069-1072.
23. de Lima, M.d.F.R., et al., *Bioactivity flavonoids from roots of Euphorbia tirucalli L.* Phytochemistry Letters, 2021. **41**: p. 186-192.
24. Prasain, J.K., et al., *Metabolism and growth inhibitory activity of cranberry derived flavonoids in bladder cancer cells.* Food & function, 2016. **7**(9): p. 4012-4019.
25. Khafagy, S., Z. Mahmoud, and N.E. Salam, *Coumarins and flavonoids of Ricinus communis growing in Egypt.* Planta Medica, 1979. **37**(10): p. 191-191.
26. Singh, B., et al., *Saccharonol B, a new cytotoxic methylated isocoumarin from Saccharomonospora azurea.* Tetrahedron Letters, 2013. **54**(49): p. 6695-6699.
27. Chen, G., et al., *Isofraxidin alleviates myocardial infarction through NLRP3 inflammasome inhibition.* Inflammation, 2020. **43**(2): p. 712-721.
28. Ito, C., et al., *Antitumor-promoting activity of coumarins from citrus plants.* Planta medica, 2005. **71**(01): p. 84-87.

29. Ribeiro, P.R., et al., *Physiological and biochemical responses of Ricinus communis seedlings to different temperatures: a metabolomics approach.* BMC Plant Biology, 2014. **14**(1): p. 223.
30. Alamri, A., et al., *Effect of erucic acid against DMBA-induced breast cancer via inflammatory/apoptosis pathway.* Food Bioscience, 2025: p. 107508.
31. Ramothloa, T.P., et al., *Phytochemical composition and multifunctional applications of Ricinus communis L.: Insights into therapeutic, pharmacological, and industrial potential.* Molecules, 2025. **30**(15): p. 3214.
32. Majumder, M., et al., *Ricinus communis L. fruit extract inhibits migration/invasion, induces apoptosis in breast cancer cells and arrests tumor progression in vivo.* Scientific Reports, 2019. **9**(1): p. 14493.
33. Dhyani, P., et al., *Anticancer potential of alkaloids: a key emphasis to colchicine, vinblastine, vincristine, vindesine, vinorelbine and vincamine.* Cancer cell international, 2022. **22**(1): p. 206.
34. Tripathi, A.C., R. Gupta, and S.K. Saraf, *Phytochemical investigation characterisation and anticonvulsant activity of Ricinus communis seeds in mice.* Natural Product Research, 2011. **25**(19): p. 1881-1884.
35. Obaineh, O., A. Oluwole, and O. Adekunle, *Phytochemistry, Phenolic Contents and Free Radical Scavenging of Bauhinia thoningii kurtz and Ricinus communis L Extracts as Possible Contribution to Medicinal Effects.* British Journal of Pharmaceutical Research, 2015. **7**(1): p. 9-15.
36. Ohishi, K., et al., *Ricinine: a pyridone alkaloid from Ricinus communis that activates the Wnt signaling pathway through casein kinase 1α.* Bioorganic & medicinal chemistry, 2014. **22**(17): p. 4597-4601.
37. Misal, S., et al., *Peroxisome proliferator-activated receptor antagonists as emerging therapeutics in cancer treatment.* Bioorganic Chemistry, 2025: p. 108693.
38. Qian, Z., et al., *The emerging role of PPAR-alpha in breast cancer.* Biomedicine & Pharmacotherapy, 2023. **161**: p. 114420.
39. Wang, Y.Y., et al., *Mammary adipocytes stimulate breast cancer invasion through metabolic remodeling of tumor cells.* JCI insight, 2017. **2**(4): p. e87489.
40. Vegliante, R., et al., *Hints on ATGL implications in cancer: beyond bioenergetic clues.* Cell death & disease, 2018. **9**(3): p. 316.
41. Rai, N., V. Kailashiya, and V. Gautam, *Exploring the protective effect against 7, 12-dimethylbenz [a] anthracene-induced breast tumors of palmitoylethanolamide.* ACS Pharmacology & Translational Science, 2023. **7**(1): p. 97-109.
42. Li, H., et al., *Targeting PI3K/AKT/mTOR signaling pathway in breast cancer.* Cancers, 2021. **13**(14): p. 3517.
43. Temple, A.E. and S.R. Walker, *The Roles of STAT3 and STAT5 in Breast Cancer.* Cancers, 2025. **17**(11): p. 1781.
44. Balkwill, F., *TNF-α in promotion and progression of cancer.* Cancer and Metastasis Reviews, 2006. **25**(3): p. 409-416.
45. Coussens, L.M. and Z. Werb, *Inflammation and cancer.* Nature, 2002. **420**(6917): p. 860-867.
46. Augimeri, G., et al., *The role of PPARγ ligands in breast cancer: from basic research to clinical studies.* Cancers, 2020. **12**(9): p. 2623.

47. Mayer, I.A. and C.L. Arteaga, *The PI3K/AKT pathway as a target for cancer treatment.* Annual review of medicine, 2016. **67**(1): p. 11-28.
48. Li, Y.-J., et al., *STAT proteins in cancer: orchestration of metabolism.* Nature Reviews Cancer, 2023. **23**(3): p. 115-134.
49. Nolte, R.T., et al., *Ligand binding and co-activator assembly of the peroxisome proliferator-activated receptor-γ.* Nature, 1998. **395**(6698): p. 137-143.
50. Koh, Y.-C., C.-T. Ho, and M.-H. Pan, *Recent advances in cancer chemoprevention with phytochemicals.* journal of food and drug analysis, 2020. **28**(1): p. 14-37.
51. Jelic, M.D., et al., *Oxidative stress and its role in cancer.* Journal of cancer research and therapeutics, 2021. **17**(1): p. 22-28.
52. Dhillon, A.S., et al., *MAP kinase signalling pathways in cancer.* Oncogene, 2007. **26**(22): p. 3279-3290.
53. Feng, Z., et al., *The tumor suppressor p53: cancer and aging.* Cell cycle, 2008. **7**(7): p. 842-847.
54. Vara, J.Á.F., et al., *PI3K/Akt signalling pathway and cancer.* Cancer treatment reviews, 2004. **30**(2): p. 193-204.
55. Wieder, V., et al., *Prospective validation of the prognostic and predictive impact of uPA/PAI-1 in early breast cancer.* Breast Cancer Research and Treatment, 2026. **215**(1): p. 31.

Supplementary Files

This is a list of supplementary files associated with this preprint. Click to download.

- 2.sub.docx